Article:
Ma, CY, Liu, JJ and Wang, XZ (2016) Measurement, modelling, and closed-loop control of crystal shape distribution: Literature review and future perspectives. Particuology, 26. pp. 1-18. ISSN 1674-2001

https://doi.org/10.1016/j.partic.2015.09.014

Measurement, Modelling and Closed-loop Control of Crystal Shape Distribution: Literature Review and Future Perspectives

Cai Y. Ma[1,2], Jing J. Liu[2] and Xue Z. Wang[1,2,*]

[1] Institute of Particle Science and Engineering, School of Chemical and Process Engineering, University of Leeds, Leeds LS2 9JT, United Kingdom

[2] School of Chemistry and Chemical Engineering, South China University of Technology, Guangzhou, 510640, China

*** Correspondence author:**

Professor Xue Z Wang

Personal Chair in Intelligent Measurement and Control
Institute of Particle Science and Engineering
School of Chemical and Process Engineering
University of Leeds
Leeds LS2 9JT, UK
Tel +44 113 343 2427, Fax +44 113 343 2384, Email x.z.wang@leeds.ac.uk

&

China One Thousand Talent Scheme Professor
School of Chemistry and Chemical Engineering
South China University of Technology
381 Wushan Rd, Tianhe District
Guangzhou, PR China 510641
Tel: +86 20 8711 4000, Fax: +86 20 8711 4000, Email; xuezhongwang@scut.edu.cn

Abstract

Crystal morphology is known to be of great importance to the end-use properties of the crystal product and affect the down-stream processing such as in filtration and drying, but was previously regarded as too challenging to achieve automatic closed-loop control. As a consequence, previous work has focused on control the crystal size distribution (CSD) where the size of a crystal is often defined as the diameter of a sphere that has the same volume of the crystal. This paper reviews very promising new advances made in recent years in morphological population balance models for modelling and simulation of crystal shape distribution (CShD), measurement and estimation of crystal facet growth kinetics, as well as in 2D and 3D imaging for on-line characterisation of crystal morphology and CShD. A framework is presented integrating various components in order to achieve the ultimate objective of model-based closed-loop control of CShD. The knowledge gaps and challenges that require further research are also identified.

Keywords: Crystal Morphology, Crystal Shape Distribution, Morphological Population Balance Model, 3D Process Imaging, Closed-loop Control of Crystal Shape, Crystal Facet Growth Kinetics

1. Introduction

For particulate products obtained from crystallisation, crystal morphology is an important property as it not only directly impacts the downstream processing of the particles, but also could affect the end-use properties of the final product. Model-based closed-loop optimization and control of crystal shape for a population of crystals in a crystalliser, however, has long been considered to be too challenging to achieve mainly due to the limitations of available measurement techniques and modeling capabilities. Some people even questioned if there exists such a concept as morphology for a population of crystals: while it is known how to define the morphology for a crystal, it is not as clear how to define the morphology for a population of crystals. In recent years, there have been significant progresses in the areas of on-line measurement of crystal morphology via imaging, modelling of crystal shape distribution (CShD) using multi-dimensional and morphological population balance. In this article, CShD is used as the abbreviation of crystal shape distribution in order to differentiate from CSD since the latter is widely accepted in the crystallisation community to represent crystal size distribution where the size of a crystal is often defined as the diameter of a sphere that has the same volume of the crystal. The new developments have led to proof of concepts in model-based closed-loop automatic control of crystal shape distribution in crystallisation processes.

This review aims at not only providing a summary and critique of the relevant literature, but also presenting a framework that integrates the various components and pointing out the knowledge gaps that require attention in future research. As a result, rather than opening the review by straightforward going to discussion of the details of the individual elements, an integral framework is first presented that depicts a picture of how individual topical elements are linked together. The integral framework is schematically shown in Figure 1. The main components include:

- On-line real-time measurement of crystal shape and shape distribution using on-line 2D and 3D imaging instrument and image analysis techniques.
- Measurement of crystal faceted growth rates and growth kinetics using 2D and 3D images in crystal growth cells and stirred tanks, as well as estimation based on model identification method.
- Modelling and simulation of the dynamic evolution of crystal shape distribution (CShD) using morphological population balance models.
- Feedback and cascade control to track optimum operating conditions, as well as on-line optimum control.

The measured or estimated facet growth kinetics, i.e. the facet growth rate (m/s) as a function of such variables as supersaturation, solvent, impurity as well as crystal size, are needed by morphological population balance models (MPBMs) [1]. MPBMs can be used in multi-objective optimisation to obtain the optimum operating condition, such as an optimum supersaturation curve, that leads to the desired CShD as well as yield and other objectives. Control system configuration, e.g. simple feedback or cascade control, can be designed to track the optimum process condition such as the optimum supersaturation condition. Such a control strategy cannot however avoid batch to batch variations due to uncertainties, on-line measurement of crystal shape distribution is therefore required. Through real-time image segmentation analysis and shape reconstruction, the real-time size/shape distributions of crystals can be estimated. For example for a cooling crystallisation tracking the optimum supersaturation curve, the real-time crystal shape distribution information can be used to re-optimise the remaining optimum supersaturation curve.

Here it needs to point out that the presented framework might not be the only or best framework for integrating the topical elements together to achieve closed-loop control of CShD, and new and more innovative control framework is also open for future research (e.g. could CShD be directly used as the set point in a control configuration?), however it does help readers to understand how the individual components can be linked together in a framework for closed-loop control of CShD. It also needs to point out that the framework has not considered other factors, for example, for scale-up study in modelling large crystallisers, computational fluid dynamics (CFD) should be included and integrated with MPBMs to account for the mixing conditions. Furthermore, the framework was drawn with a batch or semi-batch stirred tank crystalliser in mind, for continuous or other types of crystallisers, amendments need to be made.

In the rest of the paper, developments in relevant elements will be reviewed. Topics will cover:

(1) the description of crystal shape and definition of crystal shape description (CShD), in Section 2,

(2) on-line measurement and characterisation of crystal shape and CShD using 2D and 3D imaging and image analysis techniques, in Section 3,

(3) morphological population balance models (MPBMs) for modelling the dynamic evolution of CShD subject to variations in operational conditions, in Section 4,

(4) direct measurement as well as model based estimation of faceted crystal growth rates and faceted growth kinetics, in Section 5, and

(5) model based optimisation and closed-loop control of CShD in Section 6.

Knowledge gaps and pointers to future research will be identified in individual sections as well as in the Final Remarks section.

2. Crystal Shape and Shape Distribution

Crystal shape variation can be due to difference in polymorph or morphology, the focus of this review is on morphology. Crystal morphology can dictate other quality measures such as the size. Crystals are particles structured with multiple facets that often have different surface chemistry and hence varied growth rates during crystallisation. This can lead to varied morphology even for the same polymorph. Previous research over the last half century on crystal morphology (or habit, shape) prediction has been mainly for single crystals. For a population of tens of thousands of crystals in a crystalliser, little work has been done on the modelling, optimisation and control of crystal morphology. Some people even argued that for a single crystal there is the concept of 'morphology', for a population of crystals, there is even no such a concept of 'morphology' or 'shape'. In this section, we will review the definition of crystal structure and morphology, as well as the concept of 'shape distribution' for a population of crystals, as these form the basis of morphological population balance modelling and shape distribution control.

2.1 Crystal structure, nucleation and shape

A crystal can be defined as a regular polyhedral solid bounded by plane faces, while the internal structure is composed of atoms or molecules arranged in a 3D repeating structure. Crystal structures can be solved through single crystal or powder X-ray diffraction studies, together with molecular modeling, which provide crystallographic information, such as unit cell parameters, atom coordinates, symmetry information and Miller Indices. It was realized that different crystal structure provides different packing arrangements to achieve minimal overall packing energy. Crystal shape or habit refers to the visible external shape of a crystal with the multiple facets. The morphology of a single crystal depends on the growth behaviour of its different crystallographic faces. With the known crystal structure of a compound, modeling software and experimental investigation can be used to study the crystal morphology and morphological changes. Detailed descriptions of various morphological modeling approaches including the geometrical Bravais-Freidel-Donnay-Harker (BFDH) [2]and energetic Hartman-Perdok [3] models and their variations [4-8], the tailor-made additive approach [4, 9, 10], and the detailed kinetic models, such as the 2D nucleation model and the BCF model [11, 12] can be found in literature.

The morphological modeling software such as HABIT95 [8], CrystalShape [13], and SHAPE (http://www.shapesoftware.com/), can be used to provide detailed information of the crystal morphology (shape) including locations of all faces (normal distances from the faces to crystal

center), and their corresponding corners with the input of crystallographic information from structure solution. The effect of additives, impurities and solvents on crystal morphology can also be predicted [10]. Single crystal experiments, such as X-ray topography are also useful to investigate crystal morphology, defect, and to verify modeling results. Recently, Singh et al. [13] developed a framework to generate morphology domains for screening crystal morphologies from crystal structures. Their morphological modelling software including CrystalShape and MorphologyDomain can be used to identify crystal shape and also morphology transformations under various crystallisation conditions.

Crystal nucleation is a complicated process and happens at molecular scale, which is directly affected by a number of crystallisation environmental parameters including temperature, temperature change, presence of impurities and seeds, solution agitation and the solvent used [14]. The widely used nucleation model is the empirical Nyvelt model and its modifications though there are advances in the investigations of crystal nucleation mechanisms using molecular modelling, quantum mechanics, and polythermal method [15]. A stochastic model was proposed to describe the dispersions in crystal nucleation and growth rates by implementing the fluctuations of density and temperature in crystallisation processes to obtain the size and shape dispersions of nuclei with the multi-dimensional maximisation of Gibbs free energy [16]. Clearly further research in this area is needed to accurately quantify the crystal nucleation mechanisms.

2.2 Crystal Shape Distribution (CShD)

Prior to the introduction of concept of crystal shape distribution (CShD), let's remind us the definition of crystal size distribution. Crystal size distribution used widely in describing the size of a population of particles or crystals is in effect a diameter distribution of spheres, each sphere has an equivalent volume of a particle or crystal (if each particle is simplified to a volume equivalent sphere). The concept of CShD can be easily understood by considering a population of crystals each having a shape of rod with a length, a width and a thickness. The shape distribution can then be described by three size distributions of the length, width and thickness. This clearly is a more accurate description of the size and shape for the population of crystals than the traditional diameter distribution. Instruments for measuring particle shape distribution or crystal shape distribution are often based on such a method, though they also use even simpler shape descriptors such as aspect ratio, maximum length etc.

For more complicated crystal structures however, such a method of shape distribution might not be the most effective. In morphological population balance models (to be reviewed in Section 4), the shape of a crystal is described by firstly defining a geometric centre then by the distance to the centre of each crystal face (details will be given later in Section 4).

Most commercial imaging instruments, either off-line or on-line, can provide some measurement of size as well as a number of shape descriptors such as roundness, contour/area, convexity, length/width aspect ratio and (diameter/maximum distance).However, simple descriptors could be insufficient in distinguishing the morphological differences unless the particles are significantly different in shape. Various shape descriptors have been developed in the last two decades, for example via deriving a new set of shape descriptors using the size measures of particles, or spectral or functional mathematical approaches such as the Fourier descriptors [1, 17]. However, with the advances of 3D shape measurement and prediction, the actual 3D particle shape could be described and determined through experiments and modelling, hence 3D crystal shape and CShD can become the direct and accurate description of particle shapes in the studies of crystallisation processes and particulate systems.

3. Online Monitoring and Measurements of Crystal Growth: Imaging and Image Analysis

On-line monitoring and control of crystallisation processes are becoming the essential elements to achieve high quality crystals with desired properties including shape and size distributions. The development of modern process analytical technology (PAT) and their application have provided very reliable measurement tools to obtain on-line values of important properties in a reactor, which formed the basic input and control variables for optimisation and control algorithms. However, the most important and also most difficult task for on-line optimisation and control of crystal shape and size distributions is the on-line measurement of crystal growth (then growth rate) of each crystal face, which is the frontline of crystallisation research. As shown in Sections 4-6, the ability of on-line, accurate measurement of crystal growth not only directly provides crystal growth kinetics for MPBMs, but also is essential to the development of real-time MPBM based feedback control strategies. Many recent researches have proved the feasibility of using high speed on-line imaging for crystal size and shape measurements, in particular for 1D and 2D characterisation [1, 17-40]. However, for on-line monitoring, optimisation and control of shape and size distributions in a crystalliser, it is essential to accurately and efficiently obtain 3D crystal information of the whole crystal population and the associated properties. Of the many techniques [1, 41-51] for the imaging and reconstruction of 3D objects, optical imaging and image analysis techniques proved to be the most promising ones for 2D shape measurements [1, 17, 19, 23, 24, 26, 29, 30, 32, 34, 37, 39, 52-54], and the techniques that are likely the most suitable ones for obtaining 3D crystal shape, hence growth rate of each crystal face, have made some advances in recent years [1, 45-50, 55, 56]. This is a very active research area with huge challenges and opportunities to innovatively develop process instrument and/or process probes

and the associated image processing and shape reconstruction software for the real-time monitoring, optimisation and control of particulate processes.

Despite its significant potential importance, the direct characterization of particle shape has been quite limited largely relying on off-line instruments and methods. For quite some time there have been no effective on-line instruments capable of providing real-time information on particle shape particularly with the capability to use during the processing of particles in unit operations such as crystallisation, precipitation, granulation and milling (dry or wet). Well-developed and studied PAT instruments such as acoustic and mid and near infrared spectroscopy, laser diffraction and X-ray diffraction have been used in process monitoring, but these techniques cannot give detailed information on particle shape though some have shown to be able to distinguish between different polymorphs with careful spectral data analysis using chemometrics. Overall, the inability in on-line measurement of particle shape has greatly restricted the development of monitoring and control of particle shape for particle formulation and processing systems. Below are the further reviews of the most promising and practically useful technique, optical imaging systems.

3.1 Two-dimensional imaging approaches

For online characterization of 2Dcrystal shape, recent studies on video imaging have attracted much attention, which resulted in the development of some new instrument products such as process vision and measurement (PVM) system (http://uk.mt.com/), particle image analyzer (PIA) (http://www.mts-duesseldorf.de/), in situ particle viewer (ISPV) (http://www.perdix.nl/), the on-line microscopy system of GlaxoSmithKline [1, 19, 57]. Several research groups across Europe, USA and Asia have explored the use of these systems for crystallisation process monitoring and control. Major pharmaceutical companies such as Pfizer, GlaxoSmithKline and AstraZeneca have shown keen interest inthis area. Scott et al. [58] used an inline camera prototype for qualitative monitoring of industrial crystallisation. Wilkinson et al. [57] from GlaxoSmithKline were also among the first researchers to study on-line imaging for monitoring crystallisation processes. Mazzotti and co-workers [23, 24] studied in situ monitoring of polymorphic transformation using focused beam reflective measurement (FBRM), PVM, Raman and ATR-FTIR spectroscopy, and also measured and monitored particle size and shape distributions of paracetamol by FBRM, in situ microscopy and image analysis techniques. Velazquez-Camilo et al. [38] applied an image fractal analysis technique to characterize cane sugar crystallisation with the images taken by an image acquisition system feeding with slurry samples from a crystalliser via a peristaltic pump. Calderon de Anda et al. [19] have investigated the use of the GlaxoSmithKline's imaging system for monitoring the crystallisation on-set and dynamic transition from one polymorph to another during crystallisation of LGA crystals. A multi-scale image analysis method [26, 59] was developed and used to derive monitoring charts [17], and then to calculate the

real-time growth rates associated with the evolution of the length and width for the needle-like β-polymorphic form of LGA [60].

Barrett et al. [25, 61] used the PVM imaging probe in the determination of the metastable zone of an inorganic compound and also for tracking the polymorphic transformation process of D-Mannitol crystals. Patience and Rawlings [18] investigated the use of the PVM for measuring the shape and size information of sodium chlorate crystals with support from Pfizer. Larsen et al. [29, 39] developed new algorithms including model-based object recognition for image analysis, and also highlighted the necessity of advances in image analysis to improve image segmentation when particle overlap is significant. Louhi-Kultanen and co-workers [31, 32] studied batch cooling crystallisation of sulfathiazole using an ATR-FTIR spectroscopy and image analysis simultaneously. Kramer and co-workers also conducted research using a prototype imaging probe, ISPV, which was also used at Leeds for the examination of particle shape and its subsequent development during crystal growth [52]. Srinivasan and co-workers [34] applied the PVM imaging probe and developed statistical monitoring graphs using the information from image analysis including multivariate image analysis [33]. Puel, Fevotte and co-workers [21, 27] used different in situ process analytical sensors including Mid-IR and Raman spectroscopy, in situ microscopy, PVM and FBRM, and image analysis techniques to measure particle size distribution and monitor crystallisation processes. Kail et al. [28] carried out process analysis using measured chord-length distribution from FBRM to obtain particle size distribution. Nagy and co-workers [62] used endoscopy-based in situ and also external bulk video imaging techniques and image analysis including multivariate image analysis, principal component analysis (PCA) and process control chart for the detection of crystal nucleation. Overall, all the existing investigations have demonstrated that imaging and image analysis is a very promising technique for on-line 1D/2Dcrystal size characterization.

Generally, the imaging system can be divided into two categories according to their camera locations: imaging probe inserted into a reactor and camera situated outside the wall of a reactor. The latter has convexity effects on the images due to the external curved reactor wall or needs an imaging window attached to the external curved reactor wall in order to minimize the effects. Furthermore, for jacketed reactors, condensation on the external wall during cooling crystallisation or bubbles in the cooling fluid can obstruct the optic pathway, hence reducing image quality. Most recently several researchers carried out investigations on crystallisation processes in reactors via installing inline imaging systems, which records crystal images using an imaging system or a microscopy with a flowcell through which crystal suspension is pumped from a reactor [23, 45, 48, 63]. The obtained images may be of better quality than an in-situ probe system, but the external flowcell loop cans easily cause cogging,

encrustation, and/or crystal breakage by the pump. This system can provide flexible arrangement among camera, light and particles in order to obtain high quality images, however, it may take a long time to tune the optic arrangement for the best configuration because the camera must focus on a small volume of slurry near the inner wall with light guide pointing at the same volume with proper illumination intensity. In contrast, imaging probe [29, 30, 39, 52, 64] can overcome these disadvantages but the feature of flexible arrangement will lose and currently the system cannot be applied to small size reactors (say 0.1litre) due to the smallest size of the probe available. The probe may only be used for short periods due to the high temperature of slurry in reactors or continuously cooling of the probe is required. Furthermore, the probe may be contaminated or encrusted during crystallisation processes, which requires the probe to be taken out from the reactors and cleaned. Overall, both imaging systems are suitable for monitoring and control of crystallisation processes in research laboratories. The probe imaging system is the most suitable one to be used in industry due to the relative less effort of setup and maintenance, also less limitations on probe size because of using larger size of reactors in product lines.

3.2 Three-dimensional imaging systems

Despite the intensive research and development programmes internationally in recent years, most of the work is restricted to 2D imaging. Although obtaining 2Dcystal shape is already a major step from the traditional characterisation of particles based only on a volume equivalent diameter of a sphere, being able to measure 3D crystal growth, hence crystal shape evolution, on-line will be of much greater scientific and industrial significance. Intensive research and development has been carried out to obtain 3D topographical data of objects in robotics and machine vision areas for applications such as vehicle identification and face recognition. In addition, research is being carried out for three-dimensional (3D) particle shape measurements [1, 30, 45, 48, 51, 56, 65], in particular the determination of crystal facet growth rates.

Confocal microscope is able to provide 3D information of a particle by scanning many thin sections of the sample, then stacking them to form a 3D particle [50]. InfiniteFocus (http://www.alicona.com/)can also carry out 3D surface measurements using vertical scanning to provide topographical and colour information from the variation of focus. However, these systems are not practical for 3D on-line measurements due to the very low speed in operation.

In medical and biological areas, CCD cameras and miniature cameras were used to develop imaging systems. Interactive systems that allow users to control and manipulate real-world objects within a remote real environment are known as teleoperator or telerobotic systems. Such systems are often used in medical applications to confirm diagnosis and make telepresence surgery. A lot of endoscopes

have been developed for these purposes (see for example [66, 67]). The most known telerobotic surgery systems are da Vinci telerobotic surgical system [66] and ZEUS [67]. Such systems are controlled by surgeons remotely by viewing virtual surgical site with stereoscopic system and controlling stereoscopic camera and robot surgical armaments. However, these imaging systems still have significant limitations in terms of their image processing capabilities and how to link the information for shape monitoring and control. In fact at the moment they are mainly used to display information to operators and store data onto hard drive.

Stereo imaging has the advantage of providing more direct, unambiguous and quantitative depth information for 3D shape reconstruction. The stereo imaging system can have different camera-object geometries such as the common parallel camera optical axes, the converging (nonparallel) camera optical axes, etc. [68]. Gorpas et al. [43] developed a volumetric method to measure small objects (ca. 10mm) using a binocular machine vision system. The system consists of two CCD cameras, telecentric lenses, and a structured light projector. Camera calibration, image pre-processing and segmentation, stereo matching and 3D coordinate calculation were performed to reconstruct 3D tumour surfaces (ca. 10 mm in size). In the study of Boersma et al. [41], the three cameras were positioned in a triangle location with a small angle for the cameras to focus on same area interested. Three image pairs were analysed using a digital surface model, and then combined to provide 3D information of a wound area. Bottlinger and co-workers [46] developed an orthogonally-positioned three-camera imaging system for measuring 3D shape of free-falling particles (100μm ~ 4mm). The reconstruction method used the boundaries of two images to build 3D wire-structure, and approximated the boundary of the third image as a polygon to stack all scaled and fitted polygons to form 3D structure. Castro et al. [44] presented a technique for determining the 3D size, shape and number density of prismatic microlites in obsidian, which involves collecting a series of optical images at successive levels in a transparent thin section with a petrographic microscope and digital camera and combining these images to form 3D stacks. The determination of embedded particles within dispersed elements in multiphase dispersions was achieved by using micro-stereoscopic on-line image acquisition technique [47]. The accurate images from a four-phase system model simulating a fermentation broth were acquired to identify and count the oil-trapped particles moving at high speed. An imaging system using a flow through cell with one camera and two mirrors was developed to obtain 3D information of crystals grown from solution [23, 48]. The optic arrangement enables the acquisition of two images from the particle at different angles, the reconstruction of 3D structure using image processing software. Zhang et al. [51] used non-invasive stereovision imaging technique to to perform on-line measurements for the accurate determination of real size and shape of crystals grown in a stirred tank crystalliser. Darakis et al. [42] presented the application of digital holography, an

effective 3D imaging technique, for the measurement of size, orientation and location of opaque micro fibres. The method can provide 3D volume information from a single hologram acquisition with the actual location of the particle being determined subsequently by reconstructing the recorded hologram at different depths, hence avoiding the problem of out-of-focus particles from classical imaging techniques. Further research is needed to explore the applicability and capability of this method to obtain 3D particle size and shape distributions in reactors. A 3D stereovision imaging system was proposed in Figures 2 and 3 and tested to obtain stereo images of crystals grown from solution for the reconstruction of 3D crystal shape [1, 51, 69, 70]. The on-line 3D imaging probe system, as shown in Figure 3, including an imaging probe, camera controllers, and, a crystalliser, image acquisition software is also being developed for the measurement of 3D crystals in reactors.

3.3 Image Analysis and 3D reconstruction

For the quantitative analysis of in-process images for process control, the first requirement is to use image segmentation to separate the crystals from the image background. Some of the most popular commercially available image analysis software such as Image Pro Plus (http://www.mediacy.com/), Quant/2 (http://www.soft-imaging.net/), Clemex Vision PE (http://www.clemex.com/), Leica Qparticles (http://www.leica-microsystems.com/), Mex (http://www.alicona.com/), HALCON 10 (http://www.mvtec.com/) can be used for such applications[1]. Overall, all of these software systems include a wide variety of image processing and analysis features, such as image enhancement, image Fourier transform processing, image filtering, morphological operations, automatic segmentation with single threshold, shape measurement and others. However, several researchers found that it is not trivial to apply these software systems directly to images obtained under an on-line process environment, e.g. for slurries of particles which are suspended in solution [19, 25, 61]. The major challenges in such situations lie in the fact that the slurries in a stirred tank reactor are in continuous motion, and that the variation of distances from the camera lens to particles captured in a snapshot makes some particles rather poorly resolved and fuzzy in definition as compared to others, reflecting the depth of focus for the microscope objective lens system. In addition, the effect of individual particle illumination as well as temporal changes of hydrodynamics within the reactor may lead to variable intensity in the image background. A multi-scale image segmentation method using wavelets for image analysis initially developed for emulsion polymerization [71] and later effectively adapted for segmentation of images obtained on-line from crystallisers using the GSK imaging system [26]. Pollanen et al. [31] also applied a similar image segmentation approach to on-line images with satisfactory results. Larsen et al. [29, 39] developed an image segmentation method for crystals with high aspect ratios which was also able to satisfy the demand of real-time use. However, for all these methods, there is still a significant challenge for high solid concentrations when crystals in an image

frame are overlapped [59]. The multi-scale image analysis approach [71] proved to be able to effectively identify the edges of particles for high solid concentrations for images of polymerization bubbles and ashes, as well as for crystallisation, work is currently being carried out in order to correctly recognize the particle objects after the edges are identified. In this respect, it is interesting to mention that high-solid concentration has also known to be a significant challenge to other process analytical instruments such as acoustic spectrometer and laser diffraction due to multiple diffraction and particle-particle interaction.

To extract 3D information from the recorded stereo image pairs for 3D reconstruction of objects, it is necessary to find disparities among a series of corresponding points between a pair of stereo images taken from the same scene. There are many matching techniques and corresponding algorithms which can be generally divided into three categories: area-based, feature-based, and their combination. Area-based algorithms use image grey level distribution information directly, to find the best match between a pair of images. Various correlation techniques are used to define area-based algorithms. Feature-based algorithms compare specific characteristics extracted from a pair of images, such as edges, lines, vertices and other regular shapes. Through this process a best match between two images can be obtained. In general, the correlation algorithms used provide for good matches, by taking advantage of their inherent noise suppression effects if distortion is not excessive. This approach may not be the best alternative when attempting the detection of the peak of a broad correlation function. Thus, feature-based algorithms strongly depend on good, noise-free images for exact feature extraction. In general, feature-based techniques yield a best match more stably and accurately than area-based techniques. Two types of features commonly used are point-like features such as corners and line segments [72]. The extracted 3D information can then be further processed to calculate the sizes and growth rates of individual faces, and to perform polymorph identification and classification and through this to develop new monitoring charts which can be used for improving quality control in manufacture. For the later purpose, shape descriptors need to be calculated.The typical 3D shape structure of a potash alum crystal grown from solution was reconstructed from 2D stereo images obtained from potash alum crystals [69]. Mazzotti and co-workers [48, 73] used a flowcell with one camera and two mirrors to generate stereo images for 3D shape reconstruction. The reconstruction ability of this method depends on the developed model and the detection of image features such as lines and corners. Alternatively, based on a camera model, the boundaries of the 2D projections from the 3D shape of a particle were obtained to form a huge 2D projection dataset [30, 45]. The experimentally recorded 2D images were then used to screen all 2D projections in the dataset to obtain the corresponding 3D shape. The accuracy depends on the generated 2D projection dataset and

crystals with different shapes may need different 2D projection datasets for their 3D shape identification.

4. Morphological Population Balance Modelling

4.1 Multi-dimensional and Morphological Population Balance Models

A population balance (PB) model generally accounts for the convective processes that involve both the motion of particles in a system through their defined domains and their birth-and-death processes that can both terminate existing and produce new particles [74]. In literature, the so-called multi-dimension is often interpreted as multiple-variables, i.e., a single-size dimension as volume equivalent spherical diameter plus other variables, such as particle location, porosity and fraction ratio. Crystal morphology has been a very important research area, but the focus has been on shape prediction for single crystals [10, 75-80] rather than for all the crystal population within a crystalliser. On the other hand, although population balance (PB) modeling for crystallisation processes is for all crystals in a crystalliser, crystal shape was often ignored with an over-simplified crystal-size definition, i.e., the volume equivalent diameter of spheres (see for example [54, 81-88]). The difference between morphological PB model and multi-dimensional (multi size dimensional) PB models for crystallisation in the published literature differs mainly in how the size dimensions are defined. The former defines the multiple size dimensions as the normal distances of each face to its geometric centre, while the later always involves some simplification e.g. simplify a crystal to plates that have only two dimensions. As a matter of fact, published literature so far on multi size dimensional PB models have been limited to two size dimensions. It is our opinion that morphological PB models have advantages over the so-called multi size dimensional PB models because the former can fully re-construct the shape(structure) of any one crystal at any time, while the later always have to simplify the crystal to a simpler structure (using e.g. characteristic sizes) so cannot fully re-construct the crystal shape. A morphological PB model is definitely a multi-dimensional PB model, but a multi-dimensional PB may not be morphological.

Recent developments in multi-dimensional and morphological PB modeling provide a promising technique for bridging morphology modeling at the two size scales: for single crystals and for the population of crystals in a crystalliser. Puel et al. [21, 89] developed a 2D PB model to predict the growth of hydroquinone by representing the rod-like crystals with two internal coordinates, i.e., the length and width of rectangular parallelepipeds. Other crystals such as potassium dihydrogen phosphate, L-glutamic acid and hen egg-white lysozyme can also be represented by two-size parameters, and thus, 2D PB models can be developed (e.g. [20, 21, 54, 74, 89-93]). By defining the size of a face as its normal distance from the geometrical center of the crystal, Ma et al. [1, 94-96]

proposed a morphological PB model to simulate the dynamic size evolution of crystal population in faceted directions. Shape evolution of 3D faceted crystals involving morphological changes was also studied in the work of Zhang et al. [80], where the entire family of possible discrete shape evolution events, such as vertices bifurcating into edges or faces were exhaustively numerated using a set of simple testable conditions. Faceted crystal shape evolution and manipulation during dissolution or growth were studied by Snyder et al. [78, 97]. Zhang and Doherty [98] developed a method to combine a separate shape evolution model [77] with a standard 1D PB model for the simultaneous prediction of crystal shape evolution and size distribution in crystallisation processes of succinic acid. Borchert et al. [99] proposed a multi-dimensional PB to extract shape distributions in a steady state continuous crystalliser for seeded and spontaneous crystallisations. Optimal control algorithms and strategies for crystal shape manipulation were explored to obtain minimum time trajectories with the temperature as the control input [100]. Optimal scenarios with subsequent growth and dissolution phases were investigated and it was found that minimum-time scenarios were composed of constant supersaturation trajectory sections. Chakraborty et al. [101] presented a PB model for morphology distribution considering the diversity of symmetry. The symmetry of a population of crystals was analyzed using group theory and the population was divided into various symmetry classes, which, in turn, is subdivided into various morphological forms. The internal coordinate vector was represented in such a way that only one internal coordinate needed to be treated dynamically for each set with all other coordinates remaining invariant during growth, which led to a very small number of dynamic internal coordinates. Therefore, the effective dimensionality of the problem became very small, allowing simulation of a population of asymmetric crystals with minimal computational effort. Other research in multi-dimensional and morphological PB modelling of crystallisation processes include the work of Majumder and Nagy [102] who studied the influence of crystal growth modifiers, Kwon et al. [40, 103] and Liu et al. [104-106] who studied the simulation, optimisation and control of protein crystals.

The generic mathematical formulation for multidimensional PB modeling, no matter employing a single-size dimension plus other external variables, or multiple-size dimensions, can be given by the following equation [74, 95]

$$\frac{\partial \psi(\boldsymbol{x},\boldsymbol{y},t)}{\partial t} + \nabla \cdot [\psi(\boldsymbol{x},\boldsymbol{y},t)\boldsymbol{v}] + \sum_{i=1}^{N} \frac{\partial}{\partial x_i}[\psi(\boldsymbol{x},\boldsymbol{y},t) g_i(\boldsymbol{x},\boldsymbol{y},t)] = B(\boldsymbol{x},\boldsymbol{y},t) - D(\boldsymbol{x},\boldsymbol{y},t) + R(\boldsymbol{x},\boldsymbol{y},t) \quad (1)$$

where **x** is the internal variable vector with n components, which can be parameters related to crystal size, shape, and other properties; **y** is the external variable vector such as spatial coordinates (y_1, y_2, y_3); ψ is the number population density function of crystals; $\bigtriangledown$ is the gradient operator for the **y**

coordinates. For the left-hand side of Eq. (1), the first term is the accumulation term of ψ; the second term denotes the convection of ψ in the **y** space with **v** being the velocity vector; the third term is the convection of ψ due to particle growth in the **x** space with g_i being the growth rate. The first and second terms on the right-hand side of Eq. (1), B(**x**, **y**, t) and D(**x**, **y**, t), represent the birth and death terms of ψ due to all the processes during crystallisation, such as aggregation, breakage, attrition, etc. (excluding nucleation), and the third term R(**x**, **y**, t), is the nucleation term. The kernels for aggregation, breakage, and nucleation, due to their complexity, are often described by semi-empirical models [107, 108]. More recently the combination of molecular modelling with detailed experiments for the development of crystal nucleation mechanisms from molecular level has attracted much attention [15]. It is our opinion that aggregation and breakage kernels could also benefit from the methodology, i.e. by integrating molecular engineering with experiments. Considering the length of the paper, a full review on how to construct accurate and reliable kernels for nucleation (homogeneous and heterogeneous), and dissolution and Oswald ripening is not included here. Readers are directed to literature [15, 79, 109, 110].

In modelling some crystallisation processes, it may be reasonable to neglect the effect of aggregation and breakage, hence a simplified version of Eq. (1) being written as

$$\frac{\partial \psi(\boldsymbol{x},\boldsymbol{y},t)}{\partial t} + \nabla \cdot [\psi(\boldsymbol{x},\boldsymbol{y},t)\boldsymbol{v}] + \sum_{i=1}^{N} \frac{\partial}{\partial x_i}[\psi(\boldsymbol{x},\boldsymbol{y},t) g_i(\boldsymbol{x},\boldsymbol{y},t)] = R(\boldsymbol{x},\boldsymbol{y},t) \quad (2)$$

In a well-mixed batch crystalliser, the influence of crystal positions in the crystalliseron population distributions can be ignored. Therefore, Eq. (2) can be further simplified as

$$\frac{\partial \psi(\boldsymbol{x},t)}{\partial t} + \sum_{i=1}^{N} \frac{\partial}{\partial x_i}[\psi(\boldsymbol{x},t) g_i(\boldsymbol{x},t)] = R(\boldsymbol{x},t) \quad (3)$$

For seeded crystallisation processes with the assumptions of negligible contributions from nucleation, breakage, aggregation etc. to the process in a well-mixed homogeneous reactor, Eq. (3) can be further simplified as

$$\frac{\partial \psi(\boldsymbol{x},t)}{\partial t} + \sum_{i=1}^{N} \frac{\partial}{\partial x_i}[\psi(\boldsymbol{x},t) g_i(\boldsymbol{x},t)] = 0 \quad (4)$$

It is worth to note that Equations (1-4) can be applied to any crystal systems with the **x** being crystal internal coordinates and/or other crystal properties. The morphology transformations can be accounted for by varying the number of internal coordinates according to the transformations [111]. Recent studies by Singh et al. [112] developed a morphology domain concept which covers all kind of morphologies of a compound, and incorporated it into a MPBM model for automatically detect and

model the morphology transformations. A short review on MPBM focused on various new applications including crystal morphology modelling, cell growth and differentiation, gene regulatory processes, and transfer of drug resistance was conducted by Ramkrishna and Singh [113].

4.2 Efficient solution of PB equations

Theoretically, Eq. (4) can be solved for crystal population distribution with the proper initial and boundary conditions, and the combination of momentum, mass and heat transfer in the particulate system, in addition to the proper functions of nucleation and growth processes in the reactor. However, analytical solutions are only achievable for a few very simple cases. Therefore, various numerical algorithms have been developed for solving PB equations such as method of moment [114-117], method of characteristics [108, 118-121], Monte Carlo techniques [122, 123], and discretization methods including finite element technique [119, 124, 125], cell average methods [107], hierarchical solution strategy based on multilevel discretization [126], method of classes [82, 95], fixed and moving pivot method [127, 128], and finite difference/volume methods [90, 119, 129-131]. Table 1 summarises these numerical solution methods with the further reviews below.

The method of moments approximates the PB distribution by its moments [114]. Under certain conditions, the moment equations are closed, that is, the differential equations for the lower order moments do not depend on values for the higher-order moments, which results in a small number of ordinary differential equations (ODEs) that can be solved efficiently and with very high accuracy using off-the-shelf ODE solvers. The main weakness of the method of moments is the moment closure conditions are violated for more complex systems. The method of characteristics [108, 118] aims to solve the PB equations by finding curves in the L-t plane that reduce the equation to an ODE. While the method is highly efficient when the physics are simple, the approach does not generalize to complex physics. Monte Carlo simulations track the histories of individual particles, each of which exhibits random behaviour according to a probabilistic model [122, 123]. Monte Carlo simulations are most suitable for stochastic PB equations, especially for complex systems, but typically very computationally expensive. In the method of finite difference/volume discretisation, the PB equation is approximated by a finite difference scheme [90, 127, 129-131]. Numerous discretisation methods for the PB equations with different orders of accuracy have been investigated and applied to various particulate systems (see for example [82, 90, 108, 129-131]). An alternative approach, high resolution finite volume method, was proposed [90, 129, 132] to provide high accuracy while avoiding the numerical diffusion (that is, smearing) and numerical dispersion (that is, nonphysical oscillations) associated with other finite difference and finite volume methods. This method has been shown to be a promising method and applied to various crystallisation systems [90, 105, 111, 129, 130] and further developed for effectively reducing the computation time using either an adaptive mesh technique

[130] through redistributing the mesh by moving the spatial grid points iteratively and obtaining the corresponding numerical solution at the new grid points by solving a linear advection equation or a coordinate transformation technique [131] which utilizes a coordinate transformation technique to convert a size-dependent growth rate process into a size-independent growth rate problem with a larger time step to be allowed.

4.3 Morphological PB model

A morphological PB model is able to incorporate more complicated crystal structures/shapes than needle-like crystals into PB modelling, therefore, can simulate the size-related dimensional evolution of crystals for each independent crystal face and is regarded as a major development in population balance modelling by Ramkrishna and Singh in their recent review article on PB [113]. In this method, the initial facet structures can be obtained through either morphology prediction or using experimental studies of single crystals. The kinetic parameters for the crystal growth rates of each face can be estimated by experimental studies including single crystal investigations and batch crystallisation using advanced techniques, such as specialized imaging and image analysis, and also by model identification techniques. The method [95] involves several steps including the identification of independent faces using the crystal morphology information, the formulation of a morphological multi-dimensional PB model, and the solution of the corresponding PB equation to predict the location variations for each independent crystal face, and the temporal reconstruction of crystal shapes during the crystallisation process with post-processing enabling extraction of shape-related crystal properties and their relationships with the operating conditions. It is worth noting that if the homogeneous conditions, and/or symmetry of crystal shape cannot be applied to one face due to variations of hydrodynamics within a reactor, and/or addition of additives and impurities into the reactor for crystal shape manipulation, that face can be treated as an independent face, which therefore can be modelled as an additional independent dimension within the morphological PB model.

From crystal morphology studies, a potash alum crystal can have a total of 26 habit faces (Figure 4), hence a geometric center can be found. The normal distance from one face to the geometric center forms one variable (dimension) for the morphological PB model (MPBM). Since some faces, such as the 8 {111} faces, are symmetry-related and supposed to have the same surrounding growth environment, hence, same growth rates, these {111} faces can be categorised as one-dimension (x) in the MPBM. Similarly, the 6 {100} faces and 12 {110} faces forms the second (y), and third (z) dimensions, respectively. Therefore, a three-dimensional MPBM, the corresponding three parameters, x, y, z, as shown in Figure 4, can be formed to simulate the morphological evolution of potash alum crystals. This complex inorganic hydrate compound, potash alum, was specially chosen in several PB studies [94-96, 111], which displays no extensive attrition and without observed significant

particle/particle agglomeration. By solving the morphological PB equation for a time interval of $\triangle t$, the growth of individual faces, {111}, {100} and{110}, can be obtained, and, hence, used to calculate the new locations of the corresponding crystal faces, with respect to their previous locations. In this the updated normal distances for the individual faces, together with their corresponding face orientation, can be used to form a set of linear equations with the solutions of these equations generating the coordinates of all the corners of the crystal. Symmetric polytopes can be used for geometric description of crystal morphology with Miller indices. The following symmetric polytope can be used to describe the crystal shape of potash alum [111]:

$$\left| \begin{bmatrix} 1/\sqrt{3} & 1/\sqrt{3} & 1/\sqrt{3} \\ 1/\sqrt{3} & 1/\sqrt{3} & 1/\sqrt{3} \\ 1/\sqrt{3} & 1/\sqrt{3} & 1/\sqrt{3} \\ 1/\sqrt{3} & 1/\sqrt{3} & 1/\sqrt{3} \\ 1 & 0 & 0 \\ 0 & 1 & 0 \\ 0 & 0 & 1 \\ 1/\sqrt{2} & 0 & 1/\sqrt{2} \\ 1/\sqrt{2} & 0 & 1/\sqrt{2} \\ 1/\sqrt{2} & 1/\sqrt{2} & 0 \\ 1/\sqrt{2} & 1/\sqrt{2} & 0 \\ 0 & 1/\sqrt{2} & 1/\sqrt{2} \\ 0 & 1/\sqrt{2} & 1/\sqrt{2} \end{bmatrix} \begin{bmatrix} x \\ y \\ z \end{bmatrix} \right| \leq \begin{bmatrix} K_1 \\ K_1 \\ K_1 \\ K_1 \\ K_2 \\ K_2 \\ K_2 \\ K_3 \\ K_3 \\ K_3 \\ K_3 \\ K_3 \\ K_3 \end{bmatrix}, \quad (5)$$

whereK_1, K_2 and K_3 are the actual normal distances from the crystal geometric centre to {111} face, {100} face and {110} faces, respectively, at a specified time during a crystallisation process. The values of K_1, K_2 and K_3 define the shape and size of a potash alum crystal, and can be used to plot potash alum crystals. The morphological PB modeling approach has been applied to various crystallisation systems for prediction and/or optimization and control of the evolution of crystal shape/size distributions with very promising results [1, 94-96, 105, 106, 111]. The results clearly demonstrated that the morphological PB models can predict crystal growth of individual faces, hence crystal shape and size distributions at different time stages during a crystallisation process.

Protein crystals have significant benefits in the delivery of biopharmaceuticals. Although many different experimental techniques have been employed to investigate protein crystallisation, the majority has focused on fundamental investigations at the molecular and single crystal levels. Studies on modeling the protein crystal growth behavior using PB are still scarce and limited to a size definition for a particle as its volume equivalent diameter of a sphere, neglecting crystal morphology information [133]. Liu et al. [105, 106] demonstrated that simulation of protein crystallisation using

morphological PB model can potentially provide a useful tool for studying the growth behavior for the whole population of crystals in a crystalliser, helping the formation and manufacture of protein crystals. The methodology for protein crystallisation process modeling has been validated with a HEW (hen egg-white) lysozyme protein as an example using literature data. Further studies [106] using morphological PB have been carried out to investigate the effect of seed loading and cooling rate on supersaturation, and crystal size and shape distributions during crystallisation processes of HEW lysozyme crystals. Growth rates of individual faces and final crystal size and shape distributions were examined under varied seeding and cooling conditions. It was found that for growth only crystallisation, desired crystal size and shape can be obtained by coordinative manipulation of the seed loading and cooling rate: low seed loading and high cooling rate lead to large crystals of low aspect ratio, but care has to be taken to avoid nucleation and major shape change such as width becoming larger than the length. The interesting results not only demonstrated the effectiveness of morphological PB simulation for protein crystallisation but also provided useful knowledge for process optimization and control.

Multi-dimensional PB models have only been investigated for crystallisation processes. Their application to processes such as granulation and milling that produce irregularly shaped particles has not been attempted. This does not imply that particle shape is not important for these processes. It is most probably because it is much more difficult to accurately define the shape of irregularly shaped particles than for crystals, and therefore, how the multi-dimensional PB models can be applied to these processes is not obvious. A new methodology for carrying out particle shape-based PB modeling was developed via using only a small number of size dimensions, but misses little particle shape information [96]. The method is based on principal component analysis (PCA), which uses principal components (PCs) to describe the particle shape so that PB modeling can be carried out in a transformed, latent variable domain, or PC space under reduced dimensions. The simulated results [96] demonstrated that morphological PB modeling can be effectively performed in the transformed, latent variable space and the complicated real particle shape at any time of simulation can be reconstructed with high fidelity from only a few PCs. Therefore, the PCA-based morphological PB approach [96] has made it potentially realistic to carry out particle shape-based PB for particulate processes with irregularly shaped particles.

Although the developed MPBM techniques represent a significant step forward, there is still knowledge gap in the prediction and measurement of nucleation. Existing models for nucleation prediction (e.g. crystal size (diameter) distribution) are largely semi-empirical, and on-line characterisation of nuclei is still difficult. Little work has been done on the prediction and measurement of the nuclei shape distribution [134]. Therefore it requires further research in this area.

5. Characterisation of Faceted Crystal Growth Kinetics

Crystal facet growth kinetics, i.e. the growth rate (m/s) of an individual face as a function of operating conditions and other factors (e.g. supersaturation, solvent, impurity, temperature, crystal size etc.), term g in equation (1), is key information in MPBMs. Crystal facet growth kinetics can be considered as such properties as equivalent to hear transfer coefficient in heat transfer, or mass transfer coefficient in mass transfer or phase equilibrium coefficients.

Methods to measure or estimate the crystal facet growth kinetics can be grouped into four techniques, as depicted in Figure 5: direct measurement in a crystal growth cell by observing the growth of a few single crystals, statistical estimation based on measurement in a stirred tank crystalliser where crystals constantly move, estimation by combining model identification, morphological PB simulation and crystallisation experiments, as well as first principle estimation.

5.1 Facet growth rates of single crystal

Morphological PB models require accurate growth kinetic equations of internal individual faces to be available. One method of obtaining crystal facet growth rate as a function of operational conditions such as supersaturation and impurity is to experimentally observe and measure the growth of a single crystal or a few crystals in a small cell using microscope as described in the work of Kitamura and Ishizu [135, 136]. A single crystal of LGA α or β form prepared by batch crystallisation was mounted in a growth cell and measurements were performed at 298K in flowing solution. The crystal size variations in individual directions were recorded by using a microscope and a video-TV system, and used to calculate faceted growth rates. The solution concentration of the flowing stream varied between different experimental runs but was kept constant for each run. Therefore the faceted growth rates can be linked with solution concentration (supersaturation). Durbin and Feher [137] constructed a flow system to measure protein crystal growth rates under well-defined conditions. The protein solution in the system was recirculated by a peristaltic pump through a glass crystallisation cell with continuous filtration. The cell was flat with typical inner dimension of 0.6 mm × 6 mm × 20 mm, and mounted on the temperature-controlled stage of an inverted microscope equipped with a video camera and a time-lapse recorder. The solution temperature in the crystallisation cell was maintained at 24^{o}C with the average flow velocity in the cell being 0.15 m/s. Crystals were nucleated and grew to a size of 50 ~ 100 μm in am unstirred solution, then protein solution at the desired concentration was flew through the cell for crystal growth measurements. The experiments obtained growth rates of HEW lysozyme for different crystallographic faces. The growth rates obtained from this type of experiments are based on single crystal or few crystals, which differs from the operating conditions in crystallisers. In addition, the small size of such cell makes it difficult to continuously monitor and measure

concentration e.g. by putting an ATR-FTIR probe into it. New generation of growth cell system is being developed to measure faceted growth rates of crystals and also record the evolution of crystal shape with option for in-situ solution concentration measurements [70] . Figure 6 shows example images of crystal growth in a cell captured by individual 2D cameras of a stereo vision imaging system for a chemical and a protein and 3D shape reconstructed for the protein crystal. The polar plots of crystal dissolution rates were experimentally determined from the recorded crystal images during the dissolution of a single crystal in a hot-stage system [110]. The study demonstrated that polar plots method can be used to obtain the crystal evolution during growth and dissolution, and their rates of individual faces. Doherty and co-workers also developed some theoretical methods to predict crystal growth, dissolution and the effect of additives on crystal habit [76, 109, 138].

With the recent development of 3D imaging and image analysis for 3D shape reconstruction as discussed in Section 3, the accurate measurements of individual face evolution of single crystals and their faceted growth kinetics in solution can be carried out using a stereovision imaging system integrated with a growthcell set-up as described in [1]. The growthcell system has a jacketed reactor with a volume of 150 mL and the solution height of the reactor being about 20 mm. The flat cover of the growthcell is made of high-transmission and low reflection silicon glass to allow maximum light passing through it without light intensity reduction, and also has several ports for installing measurement probes including a PT100 probe for temperature, an ATR-FTIR probe for solute concentration, a pH probe, and also a port for adding seeds if necessary. The flat bottom of the growthcell allows single crystals laying on it and also avoids light diffracting. The solution temperature in the growthcell is controlled by the circulating liquid from a Julabo heating/cooling circulator. The growth process of the single crystals (from seeds or spontaneous nucleation) is recording by the 3D stereovision imaging system and the recorded stereo images are then going through the image processing steps at each processing time including image multi-scale segmentation, crystal edge/corner identification and correspondence, and stereo triangulation for 3D coordinates calculations. The 3D shape and size of each single crystal reconstructed for the whole processing period can directly be used to calculate the size evolution of each face (hence crystal shape evolution) and the faceted growth rates. Combining with the measured solute concentration using the FTIR probe will produce the crystal faceted growth kinetics. In a special case with a particular compound [65], a hot-stage reactor with a 2D imaging system produced the faceted growth kinetics with the help of some special mathematical manipulations. It should be noted that in these cases the single crystals are assumed to be stationery or move within the camera view field very slowly, which means that the solution in the growth cell is stirred at a zero or very low speed, hence the boundary layers surrounding the single crystals being thicker than that in a practical crystalliser. Therefore the

obtained face growth kinetics may not accurately represent that in a reactor. Further research is definitely needed to take into account the effect of the hydrodynamics and mixing in a crystalliser on the faceted growth kinetics. As the faceted growth kinetics is directly affected by the solute concentration on each face, the actual characteristics around the single crystals will play an important role in accurate determining faceted growth kinetics and can be simulated by computational fluid dynamics (CFD) with the solute transport modelling. Therefore the integration of molecular simulations, CFD with mixing modelling and single crystal growth experiments with stereovision 3D imaging techniques will provide more realistic and accurate facet growth kinetics.

5.2 Growth rate estimation of crystals grown in reactors

Some studies were carried out with success in literature [19, 60] to obtain facet growth kinetics using on-line imaging for real-time characterisation of particle shape. A feasibility study was conducted to estimate the growth rates of needle-shaped β-form LGA crystals in two dimensions in a crystalliser under a cooling rate of 0.1^{o}C/min [60]. Under the experimental operating conditions, the length growth rate was estimated as between 2.44 $\times 10^{-8}$ and 3.0 $\times$ 10^{-8} m/s, while the growth rate for the width is between 0.558 $\times$ 10^{-8} and 0.502 $\times$ 10^{-8} m/s. If a semi-empirical kinetic model is used, the obtained kinetic parameters are close to a dislocation-controlled mechanism [12]. This proof of concept study demonstrates that it is possible to measure real-time crystal growth of individual faces. For a given crystal polymorph with a structure more complicated than needle-like, the size of an individual face can be defined with the distance of that face from the crystal centre as shown in Figure 4. The growth rate of each face can be estimated according to the variation of size distribution in the corresponding facet direction. To obtain the faceted size distribution, it is necessary to accurately measure crystal shape using 3D imaging system, image analysis and reconstruction. For growth rate measurement of individual faces in a reactor based on on-line imaging, a time window is used, i.e. using images not only at the current time but also those before the current moment, the window width can be defined by users [60, 70]. Although some advances have been made [45, 50, 64, 65, 69, 73, 139, 140], further research is definitely needed to address this issue, and also the effect of secondary nucleation, breakage/aggregation, high-solid concentration, and co-existence of multiple polymorphic forms on accurate estimation of facet crystal growth rates.

Crystal growth rate can be affected by many factors including solution temperature, cooling rate (supersaturation), seeding (amount, size distribution), impurities, secondary nucleation, breakage and aggregation etc., which makes it very difficult to carry out direct measurement and model identification studies in a serial pattern due to the lack of precise control of all the factors between experiments. This kind of studies is also very time-consuming and cost. Therefore, for the efficient estimation of faceted crystal growth rates, high throughput (HT) techniques can play an important role

in precisely controlling the process operating conditions. The growth system constructed by Durbin and Feher [137] used 4 flowing growth cells which, however, could not be individually controlled to provide different profiles for temperature, velocity etc. Talreja et al. [141, 142] developed a kinetic model capable of predicting changes in the number and size of protein crystals as a function of time under continuous evaporation, and tested the model with experimental crystal growth data of HEW lysozyme using a HT crystallisation platform with 2 × 5 crystallisation compartments. The predicted and observed rates of crystal growth are in excellent agreement, which suggests that kinetic constants for nucleation and crystal growth for different proteins can be extracted by applying a kinetic model in combination with observations from a few evaporation-based crystallisation experiments. However, the feasibility of applying HT crystallisation equipment and/or microfluidic techniques to study crystal growth and nucleation processes of organic fine chemicals, in particular involving additives, has rarely been investigated.

5.3 MPBMs based model identification for estimation of crystal facet growth rates and kinetics

Model identification is an attractive alternative for obtaining crystal growth kinetics, and has been studied in 1D PB modelling [88, 143-145]. In applying model identification approach to 2D PB modelling, Braatz et al. [146] applied 2D PB model experiment data collected by in situ ATR-FTIR spectroscopy. Oullion et al. [20, 147] also investigated 2D crystal growth model by minimizing the error between the simulation results and experimental data in-situ ATR-FTIR spectroscopy and off-line imaging analysis. In their work, to obtain the intermediate crystal shape information, a sampling chamber was used to collect the crystals and they were then washed with fresh water, dried under vacuum. Some of the crystals were selected for image analysis. One group of kinetic parameter was obtained for further analysis of the secondary nucleation mechanism. Hu et al. [143] developed a optimisation-based approach to estimate the kinetic parameters of crystal nucleation and growth from batch cooling experiments of ammonium sulphate. The kinetic parameters were estimated using the crystal size distribution of final-time product, the initial concentration and the experimental temperature profile collected on-line in the batch crystallisation process, and in good agreement with results from other publications. Abbas and co-workers presented a method for the modelling and identification of antisolvent crystallisation kinetics of sodium chloride [145] and also ammonium sulphate kinetics for crystallisations under cooling mode [144].

The method for identification of crystal facet growth models can have the following steps [64]: (1) characterization of the shape distribution of seed crystals; (2) performance of crystallisation experiment in a crystalliser with operating conditions measured e.g. supersaturation and cooling rates; (3) characterization of the shape distribution of the product crystals at the end of the crystallisation experiment; (4) obtaining the shape distribution data from the seed crystals and product crystals

measurement, and applying the morphological PB equations to fit the parameters of the facet growth kinetics models through optimization; (5) validating the facet growth kinetic models and morphological PB models using further crystallisation experiments. In model identification based on morphological population balance models, the measurement variation can be minimised by selecting sufficiently large size of particle samples, following exactly the same experimental procedure in characterising the shape distributions of seeds and final products, and by repeating a measurement several times in steps (1) and (3). These measures can help but more rigorous statistical methods such as leave one out technique should be used to ensure the confidence in parameter estimation, but not yet reported in literature. In the study [64], different PAT sensors were used including ATR-FTIR spectroscopy for concentration measurement, turbidity probe, thermocouples, and on-line high-speed camera imaging system. The shape and size distributions of the added seeds and the dried product crystals of β-form LGA obtained at the end of the crystallisation process were characterised by the Malvern PharmaVision system 830 [64], an image-based particle analyser that allows the collection of image data of particulate materials. For the seeded cooling crystallisation process of LGA β-form crystals, nucleation, breakage and agglomeration were assumed to be negligible. Therefore Eq. (4) with N = 2 can be used to model the LGA crystallisation process with the growth kinetic parameters:

$$G_L = k_{g_L}\sigma^{g_L}\mathrm{L}^{q_L},\ G_W = k_{g_W}\sigma^{g_W}\mathrm{W}^{q_W} \quad (6)$$

To optimize the growth kinetic parameters in Eq. (6), $\theta = [k_{gL}, g_L, q_L, k_{gW}, g_W, q_W]^T$, the errors between the model-predicted data and the experiment data were minimized with the objective function as follows:

$$\mathrm{Obj}(\theta) = \lambda_c\varepsilon[\sigma(\theta)] + \lambda_f\varepsilon[f_m(\theta)] \quad (7)$$

Where $\varepsilon[\sigma(\theta)]$ and $\varepsilon[f_m(\theta)]$ are the quadratic error between the measured and model-predicted solute concentration and shape number fraction of particles respectively. λ_c and λ_f are empirical scalars, which were set as to balance the respective weights of the two criteria in the computed value of Obj(θ).The minimisation of objective function was calculated by a nonlinear least-squares Levenberg-Marquardt optimisation algorithm and the results are in good agreement with those in literature [64].

For an irregularly shaped particle, although several hundred size dimensions might be required to faithfully represent its shape and size, the size dimensions can still be reduced to a significantly smaller number of PCs, in the same way as reducing from 26 size dimensions to three PCs [96]. Therefore, model identification can be used to determine the growth rates of individual PCs, hence growth rates in faceted directions. Of course, there will be anticipated and unexpected new issues arising that have to be resolved to apply the proposed method to processes handling irregularly shaped

particles. An example of these issues is that the method requires the number of original descriptors representing shape and size for all particles, large or small, to be the same. These issues will need new research but the new PB modeling methodology proposed in the article has laid the foundation forward for future investigations.

5.4 Crystal morphology prediction for growth rate estimation

Crystallisation is a very important but complicated technique with many characteristics of the compound including polymorph, shape and size, purity and stability, etc. being established during the process [109]. However, due to the lack of in-depth understanding of the crystallisation process, in particular the growth and dissolution mechanism, and the effect of additives, impurities, solvents on the crystal growth in individual face directions, the accurate manipulation and control of crystal shape is still in the very early stage. A crystal is an ordered 3D array of elements (molecules, atoms, ions) in a long-range order and crystal shape is determined by the relative normal distances of each crystal faces. Early studies related faceted crystal growth to either crystal structure or the attachment energy of the crystal. The real growth process of a crystal face from solution can include the following steps [109]: a) transporting solute molecules from bulk solution toward the face; b) diffusing the molecules on the crystal face; c) desolvating the surrounding solvent molecules at the kink sites; d) incorporating the solute molecules into the kink sites; e) releasing the latent heat of crystallisation to the crystal and solution. The modified and extended BCF growth models [148] improved the capability of mechanistic prediction of crystal morphology including the concept of kink rate, in addition to the kink density, the theory of stable and unstable edges to account for both centrosymmetric and noncentrosymmetric growth units. The approach produced excellent agreement between the predicted crystal shapes and the experimental shapes for complex systems such as paracetamol and lovastatin [109, 138]. With the advances in molecular modelling, a breakthrough in the field of crystal growth may happen and the faceted growth rates of a crystal could be accurately predicted for real complex crystallisation systems.

6. Optimisation and Control of Crystal Shape and Size Distributions

Although the focus of the review is on crystal shape distribution (CShD), it is helpful to firstly review previous work on crystal size distribution (CSD), since the methods can be adapted to CShD.

6.1 Optimisation and control of crystal size distribution (CSD)

In cooling crystallisation processes, solution temperature is reduced at a rate to generate and maintain certain supersaturation levels. If supersaturation is too large, unstable polymorphs become more likely and the nucleation rate increases which favours the formation of smaller crystals and a broader size

distribution. Higher supersaturation is necessary to cause crystallization to commence and to avoid the economic cost of longer process times. It is also common to avoid nucleation by seeding with crystals of the desired polymorphic form, which will then grow. A large number of papers about crystallisation process control have focused on the control of some properties (e.g., weight, mean, size, aspect ratio) of the CSD [84, 85, 149-151]. Fujiwara et al. [151] reviewed the application of the first-principles and direct design methods to optimize and control pharmaceutical crystallisation processes. Either approach can be implemented with concentration-vs-temperature or temperature-vs-time setpoints, with these implementations having very different sensitivities to disturbances such as deviations in seed characteristics and changes in the contaminant profiles in the feed streams. In order to control the crystal size distribution, most of the theoretical or direct design methods focus on the significant driving force, supersaturation. Studies have been made to produce crystals with different size properties through supersaturation control using ultrasonic [152], ATR-FTIR [153]. Until now, supersaturation control has been successfully used to obtain narrow particle size distributions [154]. Recently, precision manufacture of crystalline products with desired shape demands on-line techniques for real-time monitoring and control of the evolution of crystal morphology [19]. There is some work regarding the methods to modify the crystal size by controlling the supersaturation level during crystal growth [18, 155] or by using impurities to manipulate the shape of crystals for sodium chlorate, which also represents an important direction since the use of impurity is considered in industry as an effective handle for size control. Several studies were carried out to develop some robust closed-loop control strategies (for example [1, 64, 139, 156-160]) with the help of the advanced in-situ sensors developed in last decade. But very few are based on proper design of feedback control system to achieve the crystal population shape.

Most of the optimal operation profiles based on the first principle method are generated from the population balance model. Traditionally the stopping criterion for model accuracy has been based on engineering guesswork [161]. A data-efficient method for model development is an iterative procedure involving optimal experimental design, automated batch experiments, parameter estimation, and model selection [162]. Once the model is sufficiently accurate, a dynamic optimization algorithm can be used to compute the physical design variables, initial conditions, startup procedures, setpoints to lower level feedback control loops, and the feedback control system. Several optimal control algorithms have been developed to provide robustness to parameter and control implementation uncertainties [151, 163]. Costa et al. [164, 165] considered a procedure to minimize standard deviation of the final CSD using the successive quadratic progeamming coupled with the discretisation of the control variables, and also the generic algorithm coupled with parameterization of the control variables. Mazzotti et al. [166, 167] used model-based optimization techniques to control CSD in

batch cooling crystallisation of paracetamol in ethanol and also the combined cooling/antisolvent crystallisation of acetylsalicylic acid in ethanol-water mixtures. Rohani and co-workers (see for example [168-174]) minimized the optimization objective function with respect to a parameter vector temperature input, subject to the mass balance dynamics as well as the PB equation to obtain optimal cooling policy for product quality control. They also developed real-time model-based optimal control of anti-solvent semi-batch crystallisation processes and seeded batch crystallisation processes using real-time single and multi-objective optimization, rigid logic and fuzzy logic control methods [171-175]. Kramer and co-workers [158, 176] applied dynamic optimization for throughput maximization of an industrial semi-batch crystallisation process with a control strategy based on a non-linear moment model and the resulting problem being solved by a non-linear programming algorithm. Shi et al. [91, 133] developed a hybrid predictive control strategy using logic-based switching between model predictive control and a fall-back bounded controller with a well-defined stability region. The study demonstrated the effectiveness via the reduction of total volume of fines compared to a linear strategy, and also the robustness with respect to modeling errors.

The vast majority practice in the pharmaceutical industry use trial-and-error to experimentally determine an operating profile which lies within the metastable zone and gives acceptable crystals. A much more efficient approach is direct design, which uses feedback control to follow a setpoint supersaturation curve in the metastable zone without accurate kinetics requirement. The method has been studied in the literature (see for example, [150, 151] with a cascade control scheme being used for the concentration control and ATR-FTIR for the concentration measurement. The closed-loop control strategy used to implement direct design is most accurately referred to as concentration (or supersaturation) control. Nagy and co-workers [159, 177] used temperature cycling and optimal seed recipe with model-based optimization control strategy for crystal size distribution control of seeded batch cooling crystallisation processes. The optimization process uses PB equations with both open-loop and closed-loop schemes being evaluated. Tan and co-workers [157, 178] applied seeding and constant supersatuation control strategy using ATR-FTIR and also internal seeding technique in anti-solvent crystallisation to achieve consistent product quality including purity and CSD. Braatz and co-workers [179] compared simulations and experiments between the classical temperature control approach with the concentration-control approach. The latter approach, which uses PAT concentration measurement instrument such as ATR–FTIR spectroscopy and feedback control to follow a setpoint trajectory in the solution concentration as a function of temperature, results in reduced sensitivity of the product quality to certain disturbances. The concentration feedback control [180-182] was applied to batch cooling crystallisation of LGA for the selective crystallisation of the metastable α–form, and

also anti-solvent batch and semi-batch crystallisation of paracetamol crystals with experimental evaluation.

Detailed simulation and experimental studies showed that by controlling concentration instead of temperature profile, the control strategy can have much lower sensitivities to most practical disturbances and to variations in the nucleation and growth kinetics [183]. Barrett et al. [61] proposed an approach to use solute-specific ATR-FTIR absorption peak heights for solute solubility and dissolved concentration, in turn, supersatuation, for the optimization of cooling crystallisation processes. Louhi-Kultanen and co-workers [155, 156, 184, 185] investigated the feedback control of a reactive semi-batch precipitation process of LGA, and proposed a control structure to control the driving force of the reactive crystallisation using the feeding rate of the added acid. The solution concentration, obtained from PAT instruments such as MID-IR and ATR-FTIR, and pH were used to calculate the feedback information in the closed-loop control of the process. The developed feedback process control strategy provided effective control to form the desired polymorphs.

6.2 Crystal shape optimisation and control using MPBMs

Morphological PB model describes the dynamic evolution of particle shape as well as particle-size distribution for all crystals in a crystalliser as a function of the operational conditions, i.e., supersaturation or reactor temperature, therefore, an optimal supersaturation or temperature profile can be derived, which can lead to desired particle shape and size distribution. This provides a feasible mechanism for crystal shape control that can be easily implemented because an optimal temperature or supersaturation profile can be tracked by a simple feedback or a cascade control system through manipulating the coolant flowrate in the reactor jacket.

For potash alum crystals as shown in Figure 4, suppose the desired shape for the crystals are

$$x/y = a_1,\ y/z = a_2 \tag{8}$$

where a_1 and a_2 are the desired aspect ratios between x and y, y and z, respectively.

Then the optimization problem can be formulated as

$$\min_{r(t)} \sum_{x,y,z} \left\{ \psi\left(x, y, z, t_f\right) \left[\left(x/y - a_1\right)^2 + \left(y/z - a_2\right)^2 \right] \right\} / \sum_{x,y,z} \psi\left(x, y, z, t_f\right) \tag{9}$$

subject to

$$r_L \le r(t) \le r_U \tag{10}$$

where r(t) is the cooling rate with the lower bound r_L and the upper bound r_U; $\sum_{x,y,z}\psi(x, y, z, t_f)$ corresponds to the sum of all number population densities at t= t_f across the discrete grid of the whole parameter space; and $\psi(x, y, z, t_f)$is the predicted final number population density function using the morphological PB model. Apparently, except for the imposed constraint on cooling rates (Eq. (10)),there are many other ways to define objective functions concerning particle shape, size distributions and all the morphological forms, such as state constraints for specifying the crystal shape and size distribution to formulate a typical model predictive control scheme [91, 133].

Optimization is performed using Eq. (9) as the objective function and setting $a_1 = a_2 = 1$. An optimal temperature profile and the corresponding supersatuation trajectory can be obtained with the pre-defined lower and upper bounds of the cooling rate. The shape evolutions of a potash alum crystal demonstrate that the initial 26 faces remain at the end of the simulation, but the shape and size in every face direction are changed. The value of $(a_1 - 1)^2 + (a_2 - 1)^2$ approaches zero as the operating condition follows the optimal supersaturation profile [111] which indicates that its morphology does grow to approach the desired morphology. This study demonstrated that the model can be used to derive optimal supersaturation and temperature profiles for a given objective function related to particle shape, hence providing a closed-loop methodology for crystal shape tailoring, which can be easily implemented via a standard feedback or cascade control system using jacket cooling water. Work has also been carried out to investigate an alternative means for manipulating faceted crystal growth by adding impurities using the morphological PB model [102, 186, 187]. The same optimization procedure has also been used for crystal shape control of LGA β-form crystals grown from solution with the growth kinetic parameters obtained from model identification [64]. Liu et al. [104] also carried out multi-objective optimization of protein crystal shape and size, in which the aspect ratio of the mean normal distances from two independent faces (101) and (110) representing 12 faces of the crystal of hen egg white lysozyme was identified as the objective function with the lower and upper boundaries of the cooling rate to constrain the optimisation. The genetic algorithm was used to perform the optimization. Christofides and co-workers [103] also investigated the modelling and control of crystal shape in continuous protein crystallisation using again the aspect ratio of mean sizes between faces (101) and (110) as the objective function. The formed objective formulation includes the weighted aspect ratio term, growth ratio term and jacket temperature change term. By adjusting the weight for each term, the unnecessary aggressive control action could be avoided.

Closed-loop control of crystal shape in a crystalliser, however, has long been considered to be too challenging to achieve mainly due to the limitations of available measurement techniques and modelling capabilities, hence its research being relatively scarce [178]. However, there have been very

promising advances recently in both on-line characterization and modelling of crystal shape evolution for crystallisation processes, which could ultimately lead to practical solutions to closed-loop shape control. Ma et al. [188] presented a methodology for crystal shape control and optimization in cooling crystallisation of potassium dihydrogen phosphate, which is based on optimizing the temperature profile and other influencing factors such as the seeding mass or the dissolution amount. A multidimensional PB model was developed in their work, which used two characteristic size dimensions to represent the shape of a twelve-faceted crystal. For the same chemical, Yang et al. [155] proved experimentally that the shape for a population of crystals was able to be tailored by manipulating the supersaturation profile. In addition to manipulating the temperature or supersaturation profile in cooling crystallisation, another means of influencing the shape of growing crystals is the introduction of impurities. An generic model control strategy for on-line dynamic optimization and batch-to-batch optimization has been studied for improving the product quality of a seeded batch cooling crystallization [189]. Patience and Rawlings [18] investigated the use of impurities to manipulate the shape of crystals for sodium chlorate, which also represents an important direction since the use of impurity is considered in industry as a very effective handle for shape control. A model predictive controller with PB modelling of protein crystallisation was used to produce crystals with a desired shape distribution [40]. Ma [190] developed a methodology to generate an optimum operation profile of a crystallisation process based on the optimization of first-principle model with the objective function being the length and width ratio for validation simplicity and the optimisation being subject to upper and lower bounds of cooling rate, operating temperature and time.

It is important to note that theoretically speaking, when the process follows the optimal temperature profile and concentration trajectory, the final product should have the size and shape distributions as the optimised targets. However, during crystallisation processes, there exist uncertain disturbances from temperature, concentration, impurities, etc., and the accuracy of modelling techniques/parameters, which can cause batch-to-batch variations even using the same optimal profiles. Therefore it is crucial to introduce on-line MPBM-based optimization method to continuously update the crystal size and shape evolution with other monitoring parameters. This will bring the crystallisation process to the trajectory for the desired final product with optimal characteristics. As the on-line optimization technique requires the MPBM-based optimization to be carried out for each update, the solution speed may affect how frequently the update can be performed. Higher frequency of the update and re-optimisation, higher chance obtains the desired product. However, the optimization based on MPBM is time consuming, further research is needed to improve

computational speed with faster processors, parallelised algorithms, better optimisation solution techniques etc.

It also needs to be mentioned that the optimization techniques used for crystallisation processes are only based on the mean size (diameter or faceted) of crystals, not the real crystal shape distributions as they normally did not include the other distribution parameters such as standard deviation if a normal (Gaussian) faceted size distribution can be used to represent the actual distribution. When using a target shape as the objective function, the mean sizes of individual faces from their size distributions or the ratios between the mean sizes at each optimizing time are normally used as the optimization variables as described in literature [103, 104, 111]. If the shapes of size distribution for individual faces are conserved during the crystallisation processes, for example the crystal growth from solution is dominated by pure growth mechanisms with little effects from size itself, secondary nucleation, aggregation and breakage, the standard deviation for each size distribution of a crystal face will be kept the same over the whole crystallisation process. Therefore the mean sizes or their aspect ratios could truly represent the evolution of each size distribution in population, hence the shape distribution of crystals in the entire crystalliser. However, in most practical crystallisation processes, the inclusion of secondary nucleation, agglomeration and breakage phenomena can lead to the variation of standard deviation of each faceted size distribution during crystallisation process. This will require the optimization technique to take into account each standard deviation in addition to their corresponding mean size for each face, hence forming a real multi-objective optimization problem.

It is important to note that growth rate dispersion due to size dependence and/or crystal imperfection such as dislocation and/or solvent inclusion etc. will directly affect the optimization and control of crystal shape/size distributions, and also morphology transformations. The theoretical prediction and experimental measurements of crystal growth rates and the rate dispersions can provide crucial input to the MPBM modelling for control of crystal evolution in reactors.

6.3 Manipulated variables for crystal shape optimisation and control

As discussed in the previous sections, the successful control of objectives such as crystal size, shape, form, and purity can be achieved by using manipulated variables that affect the supersaturation level in a crystalliser. For example, cooling and antisolvent crystallisers manipulate the crystalliser temperature and solvent composition, respectively, to change the solution saturation concentration, hence the supersaturation level. In addition to supersaturation, another effective means to influence crystal morphology is the use of additives or impurities, also called crystal growth modifiers (CGM). CGMs can have strong influence on crystal growth, production throughput, yield and robustness of formulations. The presence of CGM can change the surface chemistry of crystals growing from

solution, resulting in changes of the relative growth rates of the individual crystal surfaces, leading to changes in crystal shape as well as size distribution of final crystalline products. This will have profound impact on down-stream manufacturing processes such as filtration. Quantitative knowledge on their influence can be used not only to develop strategies for their removal or moderating their effects, but also to possibly make positive use of CGM as a manipulated variable for optimization and control of crystal growth processes. The effect of CGM on crystal growth, including the effects on the growth kinetics of individual faces, is a very complicated process and known to be highly selective: on the one hand, some impurity may inhibit the nucleation or growth of the crystals of one compound while promoting the nucleation or growth of the crystals of the other compound; on the other hand, the influence of the impurities on a single crystal may only demonstrate on certain crystallographic faces. Furthermore, the influence of impurities on crystallisation is also closely correlated with process environments such as supersaturation, cooling rate and pH [191]. The mechanism and kinetics for the effect of the impurities on crystallisation were studied intensively in the literature. Weissbuch et al. [192] investigated the effect of impurities on nucleation, growth and dissolution of crystals at the molecular level, and developed the tailor-made additives for blocking, docking and disrupting molecular packing arrangements during crystallisation. Molecular modelling was thereafter widely applied to explain the mechanism for the effect of the impurities on crystallisation of various compounds [10, 193]. Davey et al. [194] proposed guidelines for selecting suitable additive molecules for preventing the appearance of undesirable polymorphs by conformational mimicry. It was concluded that any successful additive molecule should have the appropriate conformation for taking part in the bonding network with minimum disruption. Along with the success of using molecular modelling to explain the mechanism for the effect of impurities on crystallisation, kinetics relating the concentration of the added impurity as well as the supersaturation and faceted growth rates of crystals was also studied in literature. Kubota and Mullin proposed a kinetic model, the Kubota-Mullin model, to describe the faceted crystal growth rate as a function of impurity concentration [195]. Kubota-Mullin model or similar kinetic models were further applied in literature to quantify the macro-scale effect of CGMs on faceted growths of various crystals including sodium chloride, hydroquinone, sucrose and LGA. Being able to model such complicated process of CGM effect for a population of crystals in a crystalliser is no doubt of great importance.

An earlier experimental study on the crystallisation of benzamide in the presence of impurities demonstrated that controlled modification of crystal habit was feasible by adding tailor-made impurities [196]. The influence of added impurities was mainly studied for single crystals to quantify the kinetic effect individually rather than for the population of crystals in the crystalliser. Patience and Rawlings [18] designed a closed-loop feedback control system for shape control in which the shape

was monitored by an imaging system, and the control was achieved by manipulating the flow rate of a habit modifier stream. Poornachary et al. [193] studied the effects of added amino acids on the habit modification in glycine crystals obtained via solution crystallisation. A molecular modelling approach using the atom-atom potential energy method is described to rationalise the experimental observations. Crystal growth is monitored in-situ using atomic force microscopy, providing insights into the interaction of impurities at the crystal-solution interfaces and consequently correlating the 'pinning' effect of impurities at the molecular scale to the macroscopically observed habit modification.

Wan et al. [186] studied the feasibility of using CGM as an additional handle (manipulated variable), in addition to cooling rates, for manipulating crystal shape distribution for a population of crystals grown from solution. Morphological PB equations were built to model the effect of L-phenylalanine, as the CGM, on the shape changing behaviour of a growing crystal population during seeded crystallisation of β-form LGA. The growth rate in the length direction is a function of CGM concentration as well as of the supersaturation, while the growth rate in the width direction only depends on the supersaturation. Both simulation and experiments demonstrated that the presence of the CGM, L-phenylalanine, inhibits the growth in the length direction, but has little effect on the width. This study provides a proof of concept of applying morphological or multi-dimensional PB models for the assessment of CGMs, and for modifying the morphology of products in relation to their commercial effect.

7. Final Remarks

The key topical areas reviewed in this paper are morphological population balance models (MPBMs), measurement and estimation of crystal facet growth rates and kinetics, on-line measurement of crystal shape and shape distribution, as well as multi-objective optimisation based on MPBMs and model-based closed-loop control of crystal shape distribution (CShD). These developments have paved the way for achieving the ultimate goal of fully automatic closed-loop control of CShD. The achievements have been reviewed. Although suggestions for future research have been made in the body of review, it is important to reiterate the key future research needs:

1. On on-line measurement of crystal shape and shape distribution, current 2D probe type imaging and non-invasive imaging instruments have provided very valuable information. There is still scope for further improvement in resolution, lighting, as well as image segmentation analysis. But clearly 2D imaging is still not satisfactory. For example, if the crystals are needle like, it is likely the length measured will be smaller than the real size. Non-invasive [69, 70] and probe like 3D imaging based on stereo vision idea holds great potential. Research on the 3D shape reconstruction algorithms to improve the accuracy, speed, robustness and tolerance to noise and image quality is needed.

2. On the measurement and estimation of crystal facet growth rates and kinetics, four approaches were reviewed (as shown in Figure 5). Direct measurement in a growth cell is particularly attractive since it promises to measure the real facet growth kinetics, just like measuring heat transfer or mass transfer coefficients. Such an instrument is under development (Figures 2 and 3) and the challenge is how to measure the solution concentration next to the crystal face since stirring can cause the crystal under observation to move. Fixed a crystal in a position is how previously people do but it means the crystal needs to be sufficiently large.

3. Study on nucleation is clearly needed in order to develop models and instruments to measure the nuclei shape and shape distribution. Current nucleation models can only predict size (diameter) distribution and are semi-empirical. On-line imaging to measure crystal shape and CShD fail when coming to the small size as nuclei. SEM, TEM and AFM microscope are difficult to be used for on-line measurement. A new nucleation model combining with molecular modelling, together with new instruments for the measurement of nucleation processes at nano-size scale is demandingly needed.

4. MPBMs need to consider aggregation and breakage phenomena, in addition to growth and nucleation. How the shape information can be used to improve the aggregation and breakage models is open for research.

5. Multi-objective optimisation based on MPBMs is time consuming. If it is to be used in on-line optimisation for on-line optimum and model-based control, research is needed to address the calculation speed issue such as through effective model reduction.

6. Integration of MPBMs with CFD models offer potentially powerful tool for scale-up and process optimization. The speed of solution and optimization will obviously become even more challenging when MPBMs are fully integrated with CFD.

7. Some laboratory based experimental studies using the approaches have been reported [51, 64], but more research on practical applications is needed.

8. The paper has presented a framework for integrating the relevant topical elements to achieve model-based automatic control of CShD. New control strategies are also open for research.

Finally, validation and application of the new methods and techniques are needed in order for them to become readily available tools that can benefit the industry.

Acknowledgments

Financial support from the following projects and organisations are acknowledged: the China One Thousand Talent Scheme, the National Natural Science Foundation of China (NNSFC) under its Major Research Scheme of Meso-scale Mechanism and Control in Multi-phase Reaction Processes (project reference: 91434126), the Natural Science Foundation of Guangdong Province (project reference:2014A030313228), the UK Engineering and Physical Sciences Research Council (EPSRC) for the projects of Shape (EP/C009541) and StereoVision(EP/E045707), and the Technology Strategy Board (TSB) for the project of High Value Manufacturing CGM (TP/BD059E).

References

[1] X.Z. Wang, K.J. Roberts, C.Y. Ma, Crystal growth measurement using 2D and 3D imaging and the perspectives for shape control, Chemical Engineering Science, 63 (2008) 1171-84.
[2] J.D.H. Donnay, D. Harker, A new law of crystal morphology extending the Law of Bravais, American Minerologist, 22 (1937) 446-67.
[3] P. Hartman, P. Bennema, The attachment energy as habit controlling factor. I. theoretical considerations, Journal of Crystal Growth, 49 (1980) 145.
[4] Z. Berkovitch-Yellin, Toward an ab initio derivation of crystal morphology, Journal of the American Chemical Society, 107 (1985) 8239-53.
[5] D.S. Coombes, C.R.A. Catlow, J.D. Gale, M.J. Hardy, M.R. Saunders, Theoretical and experimental investigations on the morphology and pharmaceutical crystals, Journal of Pharmaceutical Sciences, 91 (2002) 1652-58.
[6] R. Docherty, K.J. Roberts, Modeling the morphology of molecular-crystals - Application to anthracene, biphenyl and beta-succinic acid, Journal of Crystal Growth, 88 (1988) 159-68.
[7] X.Y. Liu, P. Bennema, Theoretical consideration of the growth morphology of crystals, Physical Review B, 53 (1996) 2314-25.
[8] G. Clydesdale, K.J. Roberts, R. Docherty, HABIT95 - A program for predicting the morphology of molecular crystals as a function of the growth environment, Journal of Crystal Growth, 166 (1996) 78-83.
[9] M. Lahav, L. Leiserowitz, Tailor-made auxiliaries for the control of nucleation, growth and dissolution of 2-dimensional and 3-dimensional crystals, Journal of Physics D-Applied Physics, 26 (1993) B22-B31.
[10] G. Clydesdale, G.B. Thomson, E.M. Walker, K.J. Roberts, P. Meenan, R. Docherty, A molecular modeling study of the crystal morphology of adipic acid and its habit modification by homologous impurities, Crystal Growth & Design, 5 (2005) 2154-63.
[11] R. Kaichew, I.N. Stranski, Zur Theorie der linearen Kristallisationsgeschwindigkeit, Z. Phys. Chem., A170 (1931) 295-317.
[12] W.K. Burton, N. Cabrera, F.C. Frank, The growth of crystals and the equilibrium structure of their surfaces, Philosophical Transactions of the Royal Society of London, 243 (1951) 299-358.
[13] M.R. Singh, P. Verma, H.-H. Tung, S. Bordawekar, D. Ramkrishna, Screening crystal morphologies from crystal structure, Crystal Growth & Design, 13 (2013) 1390−96.
[14] J.W. Mullin, Crystallization, 4th edition ed., Butterworth-Heinemann, USA, 2001.
[15] D. Camacho, A. Borissova, R.B. Hammond, K.J. Roberts, D. Kashchiev, I. Moore, K. Lewtas, Nucleation mechanism and kinetics from the analysis of polythermal crystallisation data: methyl stearate from kerosene solutions, CrystEngComm, 16 (2014) 974-91.
[16] M.R. Singh, D. Ramkrishna, Dispersions in crystal nucleation and growth rates: Implications of fluctuation insupersaturation, Chemical Engineering Science, 107 (2014) 102-13.

[17] J. Calderon de Anda, X.Z. Wang, X. Lai, K.J. Roberts, Classifying organic crystals via in-process image analysis and the use of monitoring charts to follow polymorphic and morphological changes, Journal of Process Control, 15 (2005) 785-97.
[18] D.B. Patience, J.B. Rawlings, Particle-shape monitoring and control in crystallization processes, AIChE Journal, 47 (2001) 2125-30.
[19] J. Calderon de Anda, X.Z. Wang, X. Lai, K.J. Roberts, K.H. Jennings, M.J. Wilkinson, D. Watson, D. Roberts, Real-time product morphology monitoring in crystallization using imaging technique, AIChE Journal, 51 (2005) 1406-14.
[20] M. Oullion, F. Puel, G. Fevotte, S. Righini, P. Carvin, Industrial batch crystallization of a plate-like organic product. In situ monitoring and 2D-CSD modelling: Part 1: Experimental study, Chemical Engineering Science, 62 (2007) 820-32.
[21] F. Puel, G. Fevotte, J.P. Klein, Simulation and analysis of industrial crystallization processes through multidimensional population balance equations. Part 2: a study of semi-batch crystallization, Chemical Engineering Science, 58 (2003) 3729-40.
[22] X.Z. Wang, J. Calderon De Anda, K.J. Roberts, R.F. Li, G.B. Thomson, G. White, Advances in on-line monitoring and control of the morphological and polymorphic forms of organic crystals grown from solution, KONA, 23 (2005) 69-85.
[23] M. Kempkes, T. Vetter, M. Mazzotti, Monitoring the particle size and shape in crystallization of paracetamol from water, Chemical Engineering Research & Design, 88 (2010) 447-54.
[24] M. Kempkes, J. Eggers, M. Mazzotti, Measurement of particle size and shape by FBRM and in situ microscopy, Chemical Engineering Science, 63 (2008) 4656-75.
[25] P. Barrett, B. Glennon, Characterizing the metastable zone width and solubility curve using lasentec FBRM and PVM, Chemical Engineering Research & Design, 80 (2002) 799-805.
[26] J. Calderon de Anda, X.Z. Wang, K.J. Roberts, Multi-scale segmentation image analysis for the in-process monitoring of particle shape with batch crystallisers, Chemical Engineering Science, 60 (2005) 1053-65.
[27] M. Henry, F.E. Puel, P.D. Perrichon, C. Wisniewski, G. Fevotte, Understanding and modelling of crystallization mechanisms by in-situ analytical technologies monitoring, International Journal of Chemical Reactor Engineering, 6 (2008) A3 (1-20).
[28] N. Kail, W. Marquardt, H. Briesen, Process analysis by means of focused beam reflectance measurements, Industrial & Engineering Chemistry Research, 48 (2009) 2936-46.
[29] P.A. Larsen, J.B. Rawlings, N.J. Ferrier, Model-based object recognition to measure crystal size and shape distributions from in situ video images, Chemical Engineering Science, 62 (2007) 1430 – 41.
[30] R.F. Li, G.B. Thomson, G. White, X.Z. Wang, J.C. De Anda, K.J. Roberts, Integration of crystal morphology modeling and on-line shape measurement, AIChE Journal, 52 (2006) 2297-305.
[31] K. Pollanen, A.W. Hakkinen, S.P. Reinikainen, A. Louhi-Kultanen, L. Nystrom, A study on batch cooling crystallization of sulphathiazole - Process monitoring using ATR-FTIR and product characterization by automated image analysis, Chemical Engineering Research & Design, 84 (2006) 47-59.
[32] H.Y. Qu, M. Louhi-Kultanen, J. Kallas, In-line image analysis on the effects of additives in batch cooling crystallization, Journal of Crystal Growth, 289 (2006) 286-94.
[33] D. Sarkar, X.T. Doan, Y. Zhou, R. Srinivasan, In situ particle size estimation for crystallization processes by multivariate image analysis, Chemical Engineering Science, 64 (2009) 9-19.
[34] Y. Zhou, R. Srinivasan, S. Lakshminarayanan, Critical evaluation of image processing approaches for real-time crystal size measurements, Computers & Chemical Engineering, 33 (2009) 1022-35.
[35] A. Ferreira, N. Faria, F. Rocha, S.F. De Azevedo, A. Lopes, Using image analysis to look into the effect of impurity concentration in NaCl crystallization, Chemical Engineering Research & Design, 83 (2005) 331-38.

[36] H. Ono, K. Suzuki, T. Sasaki, T. Iwato, A. Emoto, T. Shioda, K. N., Reconstruction of polarized optical images in two- and three-dimensional vector holograms, Journal of Applied Physics, 106 (2009) 083109 (1-7).
[37] L.L. Simon, K. Abbou-Oucherif, Z.K. Nagy, K. Hungerbuhler, Bulk video imaging based multivariate image analysis, process control chart and acoustic signal assisted nucleation detection, Chemical Engineering Science, 65 (2010) 4983-95.
[38] O. Velazquez-Camilo, E. Bolanos-Reynoso, E. Rodriguez, J. Alvarez-Ramirez, Fractal analysis of crystallization slurry images, Journal of Crystal Growth, 312 (2010) 842-50.
[39] P.A. Larsen, J.B. Rawlings, The potential of current high-resolution imaging-based particle size distribution measurements for crystallization monitoring, AIChE Journal, 55 (2009) 896-905.
[40] J.S. Kwon, M. Nayhouse, P.D. Christofides, G. Orkoulas, Modeling and control of protein crystal shape and size in batch crystallization, AIChE Journal, 59 (2013) 2317-27.
[41] S.M. Boersma, F.A. van den Heuvel, A.F. Cohen, R.E.M. Scholtens, Photogrammetric wound measurement with a three-camera vision system, International Archives of Photogrammetry and Remote Sensing, 33 (2000) 84-91.
[42] E. Darakis, T. Khanam, A. Rajendran, V. Kariwala, T.J. Naughton, A.K. Asundi, Microparticle characterization using digital holography, Chemical Engineering Science, 64 (2010) 1037-44.
[43] D. Gorpas, K. Politopoulos, D. Yova, A binocular machine vision system for three-dimensional surface measurement of small objects, Computerized Medical Imaging and Graphics, 31 (2007) 625-37.
[44] J.M. Castro, K.V. Cashman, M. Manga, A technique for measuring 3D crystal-size distributions of prosmatic microlites on obsidian, American Minerologist, 88 (2003) 1230-40.
[45] C. Borchert, E. Temmel, H. Eisenschmidt, H. Lorenz, A. Seidel-Morgenstern, K. Sundmacher, Image-based in situ identification of face specific crystal growth rates from crystal populations, Crystal Growth & Design, 14 (2014) 952-71.
[46] B. Bujak, M. Bottlinger, Three-dimensional measurement of particle shapes, Particle & Particulate Systems Characterisation, 25 (2008) 293-97.
[47] G. Corkidi, T. Voinson, B.I. Taboada, M.S. Cordova, E. Galindo, Accurate determination of embedded particles within dispersed elements in multiphase dispersions, using a 3D micro-stereoscopic vision system, Chemical Engineering Science, 63 (2008) 317-29.
[48] M. Kempkes, T. Vetter, M. Mazzotti, Measurement of 3D particle size distributions by stereoscopic imaging, Chemical Engineering Science, 65 (2010) 1362-73.
[49] S. Schorsch, D.R. Ochsenbein, T. Vetter, M. Morari, M. Mazzotti, High accuracy online measurement of multidimensional particle size distributions during crystallization, Chemical Engineering Science, 105 (2014) 155-68.
[50] M.R. Singh, J. Chakraborty, N. Nere, H. Tung, S. Bordawekar, D. Ramkrishna, Image-analysis-based method for 3D crystal morphology measurement and polymorph identification using confocal microscopy, Crystal Growth & Design, 12 (2012) 3735-48.
[51] R. Zhang, C.Y. Ma, J.J. Liu, X.Z. Wang, On-line measurement of the real size and shape of crystals in stirred tank crystalliser using non-invasive stereo vision imaging, Chemical Engineering Science, 137 (2015) 9-21.
[52] R.F. Li, R. Penchev, V. Ramachandran, K.J. Roberts, X.Z. Wang, R.J. Tweedie, A. Prior, J.W. Gerritsen, F.M. Hugen, Particle shape characterisation via image analysis: from laboratory studies to in-process measurements using an in situ particle viewer system, Organic Process Research & Development, 12 (2008) 837–49.
[53] C.Y. Ma, X.Z. Wang, K.J. Roberts, Multi-dimensional population balance modelling of the growth of rod-like L-glutamic acid crystals using growth rates estimated from in-process imaging, Advanced Powder Technology, 18 (2007) 707-23.
[54] A. Caillet, N. Sheibat-Othman, G. Fevotte, Crystallization of monohydrate citric acid. 2. modeling through population balance equations, Crystal Growth & Design, 7 (2007) 2088-95.
[55] J. Eggers, M. Kempkes, M. Mazzotti, Measurement of size and shape distributions of particles through image analysis, Chemical Engineering Science, 63 (2008) 5513-21.

[56] S. Schorsch, T. Vetter, M. Mazzotti, Measuring multidimensional particle size distributions during crystallization, Chemical Engineering Science, 77 (2012) 130-42.
[57] M.J. Wilkinson, K.H. Jennings, M. Hardy, Non-invasive video imaging for interrogating pharmaceutical crystallization processes, Microscopy and Microanalysis, 6 (2000) 996-97.
[58] D.M. Scott, A. Boxman, C.E. Jochen, In-line particle characterization, Particle & Particle Systems Characterization, 15 (1998) 47-50.
[59] J. Wan, C.Y. Ma, X.Z. Wang, A method for analyzing on-line video images of crystallization at high-solid concentration, Particuology, 6 (2008) 9-15.
[60] X.Z. Wang, J. Calderon de Anda, K.J. Roberts, Real-time measurement of the growth rates of individual crystal facets using imaging and image analysis: a feasibility study on needle-shaped crystals of L-glutamic acid, Chemical Engineering Research & Design, 85A (2007) 921-27.
[61] W. Su, H. Hao, M. Barrett, B. Glennon, The impact of operating parameters on the polymorphic transformation of d-mannitol characterized in situ with Raman spectroscopy, FBRM, and PVM, Organic Process Research & Development, (2010).
[62] L.L. Simon, Z.K. Nagy, K. Hungerbuhler, Endoscopy-based in situ bulk video imaging of batch crystallization processes, Organic Process Research & Development, 13 (2009) 1254-61.
[63] A. Ferreira, N. Faria, F. Rocha, J.A. Teixeira, Using an online image analysis technique to characterize sucrose crystal morphology during a crystallization run, Industrial & Engineering Chemistry Research, 50 (2011) 6990-7002.
[64] C.Y. Ma, X.Z. Wang, Model identification of crystal facet growth kinetics in morphological population balance modeling of L-glutamic acid crystallization and experimental validation, Chemical Engineering Science, 70 (2012) 22-30.
[65] C.Y. Ma, J. Wan, X.Z. Wang, Faceted growth rate estimation of potash alum crystals grown from solution in a hot-stage reactor, Powder Technology, 227 (2012) 96-103.
[66] G.H. Ballantyne, F. Moll, The da Vinci telerobotic surgical system: the virtual operative field and telepresence surgery, Surgical Clinics of North America, 83 (2003) 1293 -304.
[67] S.E. Butner, M. Ghodoussi, A real-time system for telesurgery, in: Proceedings of International conference on distributed computing systems, USA, 2001, pp. 236-43.
[68] J.F. Cardenas-Garcia, H.G. Yao, S. Zheng, 3D reconstruction of objects using stereo imaging, Optics and Lasers in Engineering, 22 (1995) 193-213.
[69] C.Y. Ma, J.J. Liu, T. Liu, X.Z. Wang, Development of a stereo imaging system for three-dimensional shape measurement of crystals, in: 25th Chinese Process Control Conf., Dalian, China, 2014.
[70] C.Y. Ma, J.J. Liu, X.Z. Wang, Stereo imaging of crystal growth, AIChE Journal, (2015) in press.
[71] J. Chen, X.Z. Wang, A wavelet method for analysis of droplet and particle images for monitoring heterogeneous processes, Chemical Engineering Communications, 192 (2005) 499-515.
[72] G. Karimian, A.A. Raie, K. Faez, A new efficient stereo line segment matching algorithm based on more effective usage of the photometric, geometric and structural information, IEICE Trans. Inf. & Syst., E89-D (2006) 2012-20.
[73] D.R. Ochsenbein, S. Schorsch, T. Vetter, M. Mazzotti, M. Moran, Growth rate estimation of β L-glutamic acid from online measurements of multidimensional particle size distributions and concentration, industrial & Engineering Chemistry Research, 53 (2014) 9136-48.
[74] D. Ramkrishna, A.W. Mahoney, Population balance modeling. Promise for the future, Chemical Engineering Science, 57 (2002) 595-606.
[75] K.J. Roberts, E.M. Walker, Predicting particle morphology on the basis of the root molecular and crystal structure, Current Opinion in Solid State and Materials, 1 (1996) 506-13.
[76] R.C. Snyder, M.F. Doherty, Predicting crystal growth by spiral motion, Proceedings of the Royal Society A, 465 (2009) 1145-71.
[77] S.B. Gadewar, M.F. Doherty, A dynamic model for evolution of crystal shape, Journal of Crystal Growth, 267 (2004) 239-50.
[78] R.C. Snyder, S. Studener, M.F. Doherty, Manipulation of crystal shape by cycles of growth and dissolution, AIChE Journal, 53 (2007) 1510-17.

[79] R.C. Snyder, S. Veesler, M.F. Doherty, The evolution of crystal shape during dissolution: Prediction and experiments, Crystal Growth & Design, 8 (2008) 1100-01.
[80] Y.C. Zhang, J.P. Sizemore, M.F. Doherty, Shape evolution of 3-dimensional faceted crystals, AIChE Journal, 52 (2006) 1906-15.
[81] J. Garside, Industrial crystallization from solution, Chemical Engineering Science, 40 (1985) 3-26.
[82] P. Marchal, R. David, J.P. Klein, J. Villermaux, Crystallization and precipitation engineering .1. An efficient method for solving population balance in crystallization with agglomeration, Chemical Engineering Science, 43 (1988) 59-67.
[83] A.J. Alvarez, A.S. Myerson, Continuous plug flow crystallization of pharmaceutical compounds, Crystal Growth & Design, 10 (2010) 2219-28.
[84] A. Gerstlauer, C. Gahn, H. Zhou, M. Rauls, M. Schreiber, Application of population balances in the chemical industry - current status and future needs, Chemical Engineering Science, 61 (2006) 205-17.
[85] M.J. Hounslow, A.E. Lewis, S.J. Sanders, R. Bondy, Generic crystallizer model: I. A model framework for a well-mixed compartment, AIChE Journal, 51 (2005) 2942-55.
[86] A.R. Menon, H.J.M. Kramer, J. Grievink, P.J. Jansens, Modelling the cyclic behaviour in a DTB crystallizer - a two-population blance model approach, Journal of Crystal Growth, 275 (2005) e1373-e81.
[87] Z. Ulbert, B.G. Lakatos, Modelling and simulation of crystallisers under non-perfect micromixing conditions, Chemical Engineering Science, 60 (2005) 3525-36.
[88] G. Fevotte, C. Alexandre, S.O. Nida, A population balance model of the solution-mediated phase transition of citric acid, AIChE Journal, 53 (2007) 2578-89.
[89] F. Puel, G. Fevotte, J.P. Klein, Simulation and analysis of industrial crystallization processes through multidimensional population balance equations. Part 1: a resolution algorithm based on the method of classes, Chemical Engineering Science, 58 (2003) 3715-27.
[90] R. Gunawan, I. Fusman, R.D. Braatz, High resolution algorithms for multidimensional population balance equations, AIChE Journal, 50 (2004) 2738-49.
[91] D. Shi, N.H. El-Farra, M. Li, P. Mhaskar, P.D. Christofides, Predictive control of particle size distribution in particulate processes, Chemical Engineering Science, 61 (2006) 268-81.
[92] K. Sato, H. Nagai, K. Hasegawa, K. Tomori, H.J.M. Kramer, P.J. Jansens, Two-dimensional population balance model with breakage of high aspect ratio crystals for batch crystallization, Chemical Engineering Science, 63 (2008) 3271-78.
[93] H. Briesen, Two-dimensional population balance modeling for shape dependent crystal attrition, Chemical Engineering Science, 64 (2009) 661-72.
[94] C.Y. Ma, X.Z. Wang, Crystal growth rate dispersion modelling using morphological population balance, AIChE Journal, 54 (2008) 2321-34.
[95] C.Y. Ma, X.Z. Wang, K.J. Roberts, Morphological population balance for modelling crystal growth in individual face directions, AIChE Journal, 54 (2008) 209-22.
[96] X.Z. Wang, C.Y. Ma, Morphological population balance model in principal component space, AIChE Journal, 55 (2009) 2370-81.
[97] R.C. Snyder, M.F. Doherty, Faceted crystal shape evolution during dissolution or growth, AIChE Journal, 53 (2007) 1337-48.
[98] Y.C. Zhang, M.F. Doherty, Simultaneous prediction of crystal shape and size for solution crystallization, AIChE Journal, 50 (2004) 2101-12.
[99] C. Borchert, D. Ramkrishna, N. Nere, A. Voigt, K. Sundmacher, On the prediction of crystal shape distributions in a steady-state continuous crystallizer Chemical Engineering Science, 64 (2009) 686-96.
[100] N. Bajcinca, V. de Oliveir, C. Borchert, J. Raisch, K. Sundmacher, Optimal control solutions for crystal shape manipulation, Computer Aided Chemical Engineering, 28 (2010) 751-56.

[101] J. Chakraborty, M.R. Singh, D. Ramkrishna, C. Borchert, K. Sundmacher, Modeling of crystal morphology distributions. Towards crystals with preferred asymmetry, Chemical Engineering Science, 65 (2010) 5676-86.
[102] A. Majumder, Z.K. Nagy, Prediction and control of crystal shape distribution in the presence of crystal growth modifiers Chemical Engineering Science, 101 (2013) 593-602.
[103] J.S. Kwon, M. Nayhouse, P.D. Christofides, G. Orkoulas, Modeling and control of crystal shape in continuous protein crystallisation, Chemical Engineering Science, 107 (2014) 47-57.
[104] J.J. Liu, Y.D. Hu, X.Z. Wang, Optimisation and control of crystal shape and size in protein crystallisation process, Computers and Chemical Engineering, 57 (2013) 133-40.
[105] J.J. Liu, C.Y. Ma, Y.D. Hu, X.Z. Wang, Modelling protein crystallisation using morphological population balance models, Chemical Engineering Research & Design, 88 (2010) 437-46.
[106] J.J. Liu, C.Y. Ma, Y.D. Hu, X.Z. Wang, Effect of seed loading and cooling rate on crystal size and shape distributions in protein crystallization—A study using morphological population balance simulation, Computers and Chemical Engineering, 34 (2010) 1945-52.
[107] J. Kumar, M. Peglow, G. Warnecke, S. Heinrich, The cell average technique for solving multidimensional aggregation population balance equations, Computers & Chemical Engineering, 32 (2008) 1810-30.
[108] S. Kumar, D. Ramkrishna, On the solution of population balance equations by discretization — III. Nucleation, growth and aggregation of particles, Chemical Engineering Science, 52 (1997) 4659-79.
[109] P. Dandekar, Z.B. Kuvadia, M.F. Doherty, Engineering crystal morphology, Annual Review of Materials Research, 43 (2013) 359-86.
[110] M.R. Singh, N. N., H.-H. Tung, S. Mukherjee, S. Bordawekar, D. Ramkrishna, Measurement of polar plots of crystal dissolution rates using hot-stage microscopy. Some further insights into dissolution morphologies, Crystal Growth & Design, 14 (2014) 5647-61.
[111] J. Wan, X.Z. Wang, C.Y. Ma, Particle shape manipulation and optimization in cooling crystallization involving multiple crystal morphological forms, AIChE Journal, 55 (2009) 2049-61.
[112] M.R. Singh, D. Ramkrishna, A comprehensive approach to predicting crystal morphology distributions with population balances, Crystal Growth & Design, 13 (2013) 1397−411.
[113] D. Ramkrishna, M.R. Singh, Population Balance Modeling: Current Status and Future Prospects, Annual Review of Chemical and Biomolecular Engineering, 5 (2014) 123-46.
[114] E. Aamir, Z.K. Nagy, C.D. Rielly, T. Kleinert, B. Judat, Combined quadrature method of moments and method of characteristics approach for efficient solution of population balance models for dynamic modeling and crystal size distribution control of crystallization processes, Industrial & Engineering Chemistry Research, 48 (2009) 8575-84.
[115] D.L. Marchisio, R.O. Fox, Solution of population balance equations using the direct quadrature method of moments, J. Aerosol Sci., 36 (2005) 43-73.
[116] M.M. Attarakih, C. Drumm, H. Bart, Solution of the population balance equation using the sectional quadrature method of moments (SQMOM), Chemical Engineering Science, 64 (2009) 742-52.
[117] S. Motz, S. Mannal, E.D. Gilles, State estimation in batch crystallization using reduced population models, Journal of Process Control, 18 (2008) 361-74.
[118] K.I. Sotowa, K. Naito, M. Kano, S. Hasebe, I. Hashimoto, Application of the method of characteristics to crystallizer simulation and comparison with finite difference for controller performance evaluation, Journal of Process Control, 10 (2000) 203-08.
[119] A. Mesbah, H.J.M. Kramer, A.E.M. Huesman, P.M.J. Van den Hof, A control oriented study on the numerical solution of the population balance equation for crystallization processes, Chemical Engineering Science, 64 (2009) 4262-77.
[120] F. Fevotte, G. Fevotte, A method of characteristics for solving population balance equations (PBE) describing the adsorption of impurties during crystallization processes, Chemical Engineering Science, 65 (2010) 3191-98.

[121] S. Mubeen ur Rehman, S. Qamar, Application of the method of characteristics to population balance models considering growth and nucleation phenomena, Applied Mathematics, 5 (2014) 1853-62.
[122] D.E. Rosner, R. McGraw, P. Tandon, Multivariate population balances via moment and Monte Carlo simulation methods: An important sol reaction engineering bivariate example and mixed moments for the estimation of deposition, scavenging, and optical properties for populations of nonspherical suspended particles, Industrial & Engineering Chemistry Research, 42 (2003) 2699–711.
[123] E.L. Haseltine, D.B. Patience, J.B. Rawlings, On the stochastic simulation of particulate systems, Chemical Engineering Science, 60 (2005) 2627-41.
[124] M. Nicmanis, M.J. Hounslow, Finite-elements methods for steady state population balance equations, AIChE Journal, 44 (1998) 2258-72.
[125] Y. Bakhbakhi, A discretized population balance for particle formation from gas antisolvent process: the combined Lax-Wendroff and Crank-Nicholson method, Computers & Chemical Engineering, 33 (2009) 1132-40.
[126] M.A. Pinto, C.D. Immanuel, F.J. Doyle, A feasible solution technique for higher-dimensional population balance models, Computers & Chemical Engineering, 31 (2007) 1242-56.
[127] S. Kumar, D. Ramkrishna, On the solution of population balance equations by discretization — I. A fixed pivot technique, Chemical Engineering Science, 51 (1996) 1311-32.
[128] S. Kumar, D. Ramkrishna, On the solution of population balance equations by discretization — I. A moving pivot technique, Chemical Engineering Science, 51 (1996) 1333–42.
[129] D.L. Ma, D.K. Tafti, R.D. Braatz, High-resolution simulation of multidimensional crystal growth, Industrial & Engineering Chemistry Research, 41 (2002) 6217-23.
[130] S. Qamar, A. Ashfaq, G. Warnecke, I. Angelov, M.P. Elsner, A. Seidel-Morgenstern, Adaptive high-resolution schemes for multi-dimensional population balances in crystallization processes, Computers & Chemical Engineering, 31 (2007) 1296-311.
[131] A. Majumder, V. Kariwala, S. Ansumali, A. Rajendran, Fast high-resolution method for solving multidimensional population balances in crystallization, Industrial & Engineering Chemistry Research, 49 (2010) 3962-72.
[132] M.W. Hermanto, R.D. Braatz, M.S. Chiu, High-order simulation of polymorphic crystallization using weighted essentially nonoscillatory methods, AIChE Journal, 55 (2009) 122-31.
[133] D. Shi, P. Mhaskar, N.H. El-Farra, P.D. Christofides, Predictive control of particle size distribution in protein crystallization, Nanotechnology, 16 (2005) 562-74.
[134] R.A. Sullivan, R.J. Davey, G. Sadiq, G. Dent, K.R. Back, J.H. ter Horst, D. Toroz, R.B. Hammond, Revealing the roles of desolvation and molecular self-assembly in crystal nucleation from solution: Benzoic and p-aminobenzoic acids, Crystal Growth & Design, 14 (2014) 2689-96.
[135] M. Kitamura, T. Ishizu, Kinetic effect of L-phenylalanine on growth process of L-glutamic acid polymorph, Journal of Crystal Growth, 192 (1998) 225-35.
[136] M. Kitamura, T. Ishizu, Growth kinetics and morphological change of polymorphs of L-glutamic acid, Journal of Crystal Growth, 209 (2000) 138-45.
[137] S.D. Durbin, G. Feher, Crystal growth studies of lysozyme as a model for protein crystallization, Journal of Crystal Growth, 76 (1986) 583-92.
[138] Z.B. Kuvadia, M.F. Doherty, Spiral growth model for faceted crystals of non-centrosymmetric organic molecules grown from solution, Crystal Growth & Design, 11 (2011) 2780-802.
[139] Z.K. Nagy, R.D. Braatz, Advances and new directions in crystallization control, Annu. Rev. Chem. Biomol. Eng., 3 (2012) 55-75.
[140] H. Eisenschmidt, A. Voigt, K. Sundmacher, Face-specific growth and dissolution kinetics of potassium dihydrogen phosphate crystals from batch crystallization experiments, Crystal Growth & Design, 15 (2015) 219-27.
[141] S. Talreja, P.J.A. Kenis, C.F. Zukoski, In situ measurement of solution concentration during the batch cooling crystallization of L-glutamic acid using ATR-FTIR spectroscopy coupled with chemometrics, Langmuir, 23 (2007) 4516-22.

[142] S. Talreja, D.Y. Kim, A.Y. Mirarefi, C.F. Zukoski, P.J.A. Kenis, 38, 988, Determination of critical supersaturation from microdroplet evaporation experiments, Journal of Applied Crystallography, 38 (2005) 988-95.
[143] Q. Hu, S. Rohani, D.X. Wang, A. Jutan, Nonlinear kinetic parameter estimation for batch cooling seeded crystallization, AIChE Journal, 50 (2004) 1786-94.
[144] A. Abbas, J.A. Romagnoli, Multiscale modeling, simulation and validation of batch cooling crystallization, Separation and Purification Methods, 53 (2007) 153-63.
[145] S.M. Nowee, A. Abbas, J.A. Romagnoli, Antisolvent crystallization: Model identification, experimental validation and dynamic simulation, Chemical Engineering Science, 63 (2006) 5457-67.
[146] R. Gunawan, D.L. Ma, M. Fujiwara, R.D. Braatz, Identification of kinetic parameters in multidimensional crystallization processes, International Journal of Modern Physics B, 16 (2002) 367-74.
[147] M. Oullion, F. Puel, G. Fevotte, S. Righini, P. Carvin, Industrial batch crystallization of a plate-like organic product. In situ monitoring and 2D-CSD modelling. Part 2: Kinetic modelling and identification, Chemical Engineering Science, 62 (2007) 833-45.
[148] A.A. Chernov, Modern crystallography III - Crsytal growth, Springer-Verlag, Berlin, 1984.
[149] A.Y. Lee, I.S. Lee, S.S. Dette, J. Boerner, A.S. Myerson, Crystallization on confined engineered surfaces: A method to control crystal size and generate different polymorphs, Journal of the American Chemical Society, 127 (2005) 14982-83.
[150] J.W. Chew, S.N. Black, P.S. Chow, R.B.H. Tan, Comparison between open-loop temperature control and closed-loop supersaturation control for cooling crystallization of glycine, Industrial & Engineering Chemistry Research, 46 (2007) 830-38.
[151] M. Fujiwara, Z.K. Nagy, J.W. Chew, R.D. Braatz, First-principles and direct design approaches for the control of pharmaceutical crystallization, Journal of Process Control, 15 (2005) 493-504.
[152] M. Schmachtl, A. Schievenbusch, G. Zimmermann, W. Grill, Crystallization process control during directional solidification in a high-temperature-gradient furnace by guided ultrasonic waves and realtime signal evaluation, Ultrasonics, 36 (1998) 291-95.
[153] H. Gron, A. Borissova, K.J. Roberts, In-process ATR-FTIR spectroscopy for closed-loop supersaturation control of a batch crystallizer producing monosodium glutamate crystals of defined size, Industrial & Engineering Chemistry Research, 42 (2003) 198-206.
[154] V. Liotta, V. Sabesan, Monitoring and feedback control of supersatuation using ATR-FTIR to produce an active pharmaceutical ingredient of a desired crystal size, Organic Process Research & Development, 8 (2004) 488-94.
[155] G.Y. Yang, N. Kubota, Z.L. Sha, M. Louhi-Kultanen, J. Wang, Crystal shape control by manipulating supersatuation in batch cooling crystallization, Crystal Growth & Design, 6 (2006) 2799-803.
[156] H. Alatalo, H. Hatakka, M. Louhi-Kultanen, J. Kohonen, S.-P. Reinikainen, Closed-loop control of reactive crystallization. Part I: Supersaturation-controlled crystallization of l-glutamic acid, Chemical Engineering & Technology, 33 (2010) 743-50.
[157] M.W. Hermanto, P.S. Chow, R.B.H. Tan, Implementation of focused beam reflectance measurement (FBRM) in antisolvent crystallization to achieve consistent product quality, Crystal Growth & Design, 10 (2010) 3668-74.
[158] A. Mesbah, J. Landlust, A.E.M. Huesman, H.J.M. Kramer, P.J. Jansens, P.M.J. Van den Hof, A model-based control framework for industrial batch crystallization processes, Chemical Engineering Research & Design, 88 (2010) 1223-33.
[159] Z.K. Nagy, Model based robust control approach for batch crystallization product design, Computers & Chemical Engineering, 33 (2009) 1685-91.
[160] X.Y. Woo, Z.K. Nagy, R.B.H. Tan, R.D. Braatz, Adaptive concentration control of cooling and antisolvent crystallization with laser backscattering measurement Crystal Growth & Design, 9 (2009) 182-91.
[161] J.B. Rawlings, S.M. Miller, W.R. Witkowski, Model identification and control of solution crystallization processes - a review, Industrial & Engineering Chemistry Research, 32 (1993) 1275-96.

[162] S.M. Miller, J.B. Rawlings, Model identification and control strategies for batch cooling crystallizers, AIChE Journal, 40 (1994) 1312-27.
[163] J.D. Ward, D.A. Mellichamp, M.F. Doherty, Choosing an operating policy for seeded batch crystallization, AIChE Journal, 52 (2006) 2046-54.
[164] C.B.B. Costa, A.C. da Costa, R.M. Filho, Mathematical modeling and optimal control strategy development for an adipic acid crystallization process, Chemical Engineering & Processing, 44 (2005) 737-53.
[165] C.B.B. Costa, R.M. Filho, Evaluation of optimization techniques and control variable formulations for a batch cooling crystallization process, Chemical Engineering Science, 60 (2005) 5312-22.
[166] C. Lindenberg, M. Krattli, J. Cornel, M. Mazzotti, J. Brozio, Design and optimization of a combined cooling/antisolvent crystallization process, Crystal Growth & Design, 9 (2009) 1124-36.
[167] J. Worlitschek, M. Mazzotti, Model-based optimization of particle size distribution in batch-cooling crystallization of paracetamol, Crystal Growth & Design, 4 (2004) 891-903.
[168] J.P. Corriou, S. Rohani, A new look at optimal control of a batch crystallizer, AIChE Journal, 54 (2008) 3188-206.
[169] Q. Hu, S. Rohani, D.X. Wang, A. Jutan, Optimal control of a batch cooling seeded crystallizer, Powder Technology, 156 (2005) 170-76.
[170] S. Rohani, S. Horne, K. Murthy, Control of product quality in batch crystallization of pharmaceuticals and fine chemicals. Part 2: External control, Organic Process Research & Development, 9 (2008) 873-83.
[171] D. Sarkar, S. Rohani, A. Jutan, Multi-objective optimization of seeded batch crystallization processes, Chemical Engineering Science, 61 (2009) 5282-95.
[172] M. Sheikhzadeh, M. Trifkovic, S. Rohani, Fuzzy logic and rigid control of a seeded semi-batch, anti-solvent, isothermal crystallizer, Chemical Engineering Science, 63 (2009) 991-1002.
[173] M. Trifkovic, M. Sheikhzadeh, S. Rohani, Kinetics estimation and single and multi-objective optimization of a seeded, anti-solvent, isothermal batch crystallizer, Industrial & Engineering Chemistry Research, 47 (2008) 1586-95.
[174] M. Trifkovic, M. Sheikhzadeh, S. Rohani, Multivariable real-time optimal control of a cooling and antisolvent semibatch crystallization process, AIChE Journal, 55 (2009) 2591-62.
[175] M. Sheikhzadeh, M. Trifkovic, S. Rohani, Real-time optimal control of an anti-solvent isothermal semi-batch crystallization process, Chemical Engineering Science, 63 (2008) 829-39.
[176] A.N. Kalbasenka, L.C.P. Spierings, A.E.M. Huesman, H.J.M. Kramer, Application of seeding as a process actuator in a model predictive control framework for fed-batch crystallization of ammonium sulphate, Particle & Particle Systems Characterization, 24 (2007) 40-48.
[177] M.R.A. Bakar, Z.K. Nagy, C.D. Rielly, Seeded batch cooling crystallization with temperature cycling for the control of size uniformity and polymorphic purity of sulfathiazole crystals, Organic Process Research & Development, 13 (2009) 1343-56.
[178] Z.Q. Yu, J.W. Chew, P.S. Chow, R.B.H. Tan, Recent advances in crystallization control: an industrial perspective, Transactions of the Institution of Chemical Engineers, 85 (2007) 893-905.
[179] M.W. Hermanto, M.S. Chiu, X.Y. Woo, R.D. Braatz, Robust optimal control of polymorphic transformation in batch crystallization, AIChE Journal, 53 (2007) 2643-50.
[180] N.C.S. Kee, R.B.H. Tan, R.D. Braatz, Selective Crystallization of the Metastable -Form of L-Glutamic Acid using Concentration Feedback Control, Crystal Growth & Design, 9 (2009) 3044-51.
[181] X.Y. Woo, R.B.H. Tan, R.D. Braatz, Modeling and computational fluid dynamics - population balance equation - micromixing simulation of impinging jet crystallizers, Crystal Growth & Design, 9 (2009) 156-64.
[182] G.X. Zhou, M. Fujiwara, X.Y. Woo, E. Rusli, H.-H. Tung, C. Starbuck, O. Davidson, Z. Ge, R.D. Braatz, Direct design of pharmaceutical antisolvent crystallization through concentration control, Crystal Growth & Design, 6 (2006) 892-98.
[183] Z.K. Nagy, R.D. Braatz, Open-loop and closed-loop robust optimal control of batch processes using distributional and worst-case analysis, Journal of Process Control, 14 (2004) 411-22.

[184] H. Alatalo, H. Hatakka, J. Kohonen, S. Reinikainen, M. Louhi-kultanen, Process control and monitoring of reactive crystallization of L-glutamic acid, AIChE Journal, 56 (2010) 2063-76.
[185] H. Hatakka, H. Alatalo, M. Louhi-Kultanen, I. Lassila, E. Haeggstroem, Closed-loop control of reactive crystallization. Part II: Polymorphism control of L-glutamic acid by sonocrystallization and seeding, Chemical Engineering & Technology, 33 (2010) 751-56.
[186] J. Wan, C.Y. Ma, X.Z. Wang, Crystal shape distribution modelling in the presence of crystal growth modifiers, in: 5th International Symposium on Design, Operation and Control of Chemical Processes - PSE ASIA 2010, Singapore, 2010.
[187] Y. Zhang, J.J. Liu, J. Wan, X.Z. Wang, Two dimensional population balance modeling of crystal growth behavior under the influence of impurities, Advanced Powder Technology, In press (2015).
[188] D.L. Ma, D.K. Tafti, R.D. Braatz, Optimal control and simulation of multidimensional crystallization processes, Computers & Chemical Engineering, 26 (2002) 1103-16.
[189] K. Patchigolla, D. Wilkinson, Characterization of organic and inorganic chemicals formed by batch-cooling crystallization: Shape and size, Industrial & Engineering Chemistry Research, 47 (2009) 804-12.
[190] C. Ma, Particle shape distribution control in crystallisation processes, PhD Thesis, in: Institute of Particle Science and Engineering, University of Leeds, 2010.
[191] K. Kadota, K. Takase, A. Shimosaka, Y. Shirakawa, J. Hidaka, Influence of habit modifiers on particle shape in a crystallization process, KONA, 24 (2006) 203-12.
[192] I. Weissbuch, L. Addadi, L. Leiserowitz, Molecular recognition at crystal interfaces, Science, 253 (1991) 637-45.
[193] S.K. Poornachary, P.S. Chow, R.B.H. Tan, R.J. Davey, Molecular speciation controlling stereoselectivity of additives: Impact on the habit modification in α-glycine crystals, Crystal Growth & Design, 7 (2007) 254-61.
[194] R.J. Davey, N. Blagden, G.D. Potts, R. Docherty, Polymorphism in molecular crystals: Stabilization of a metastable form by conformational mimicry, Journal of the American Chemical Society, 119 (1997) 1767-72.
[195] N. Kubota, J.W. Mullin, A kinetic model for crystal growth from aqueous solution in the presence of impurity, Journal of Crystal Growth, 152 (1995) 203-08.
[196] Z. Berkovitch-Yellin, J. Van Mil, L. Addadi, M. Idelson, M. Lahav, L. Leiserowitz, Crystal morphology engineering by tailor-made inhibitors: a new probe to fine intermolecular interactions, Journal of the American Chemical Society, 107 (1985) 3111-22.
[197] T.T.H. Nguyen, R.B. Hammond, K.J. Roberts, I. Marziano, G. Nichols, Precision measurement of the growth rate and mechanism of ibuprofen {001} and {011} as a function of crystallization environment, CrystEngComm, 16 (2014) 4568-86.

Table 1. Numerical solution methods of population balance equations

Algorithm	**Brief description**	**Comments**
Method of moment	To approximate the PB distribution governed by the PB partial differential equations using the moments of the distribution	• Only for very simple systems • Example references: [114, 117]
Method of characteristics	To transform high-order PB partial differential equations to ordinary differential equations with the identified curves in the L-t plane	• For simple cases • Example references: [108, 120, 121]
Monte Carlo techniques	To track the histories of individual particles subject to random behaviours	• Computationally expensive • Example references: [122, 123]
Discretisation methods	To discretise the whole range of the particle size with finite element, finite difference/volume techniques	• Numerical solution with high accuracy, low numerical diffusion and dispersion • Computational time may be an issue • Example references: [54, 82, 90, 95, 105, 108, 111, 124, 127, 129-132]
Others	To use quadrature method of moments (QMOM), sectional quadrature method of moments (SQMOM), or combine QMOM with method of characteristics	• Accurate solution with a concern of computational time • Example references: [114-117]

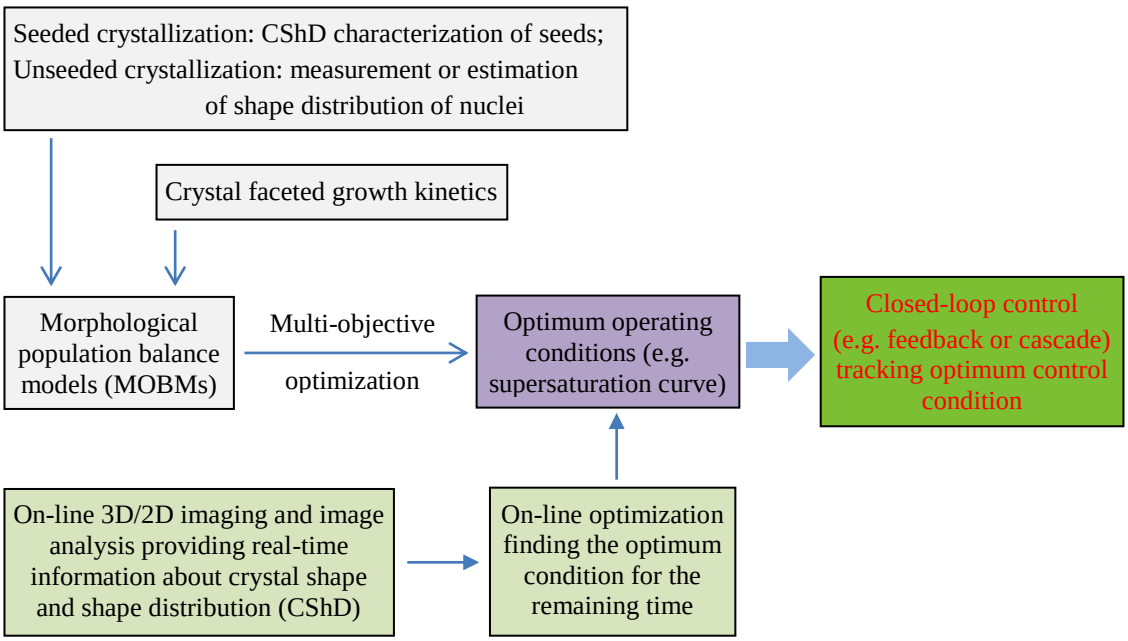

Figure 1. A framework integrating the topical elements to achieve model-based closed-loop control of crystal shape distribution in crystallisation.

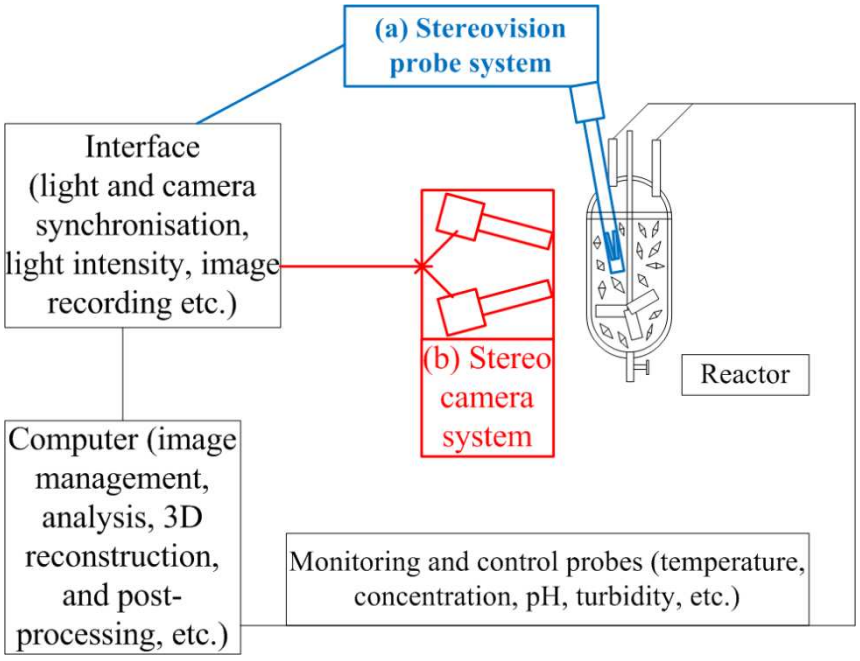

Figure 2. Conceptual layout of the stereo vision system (a) inserted into a crystalliser with a probe design (blue coloured) and (b) positioned outside of a crystalliser (red coloured).

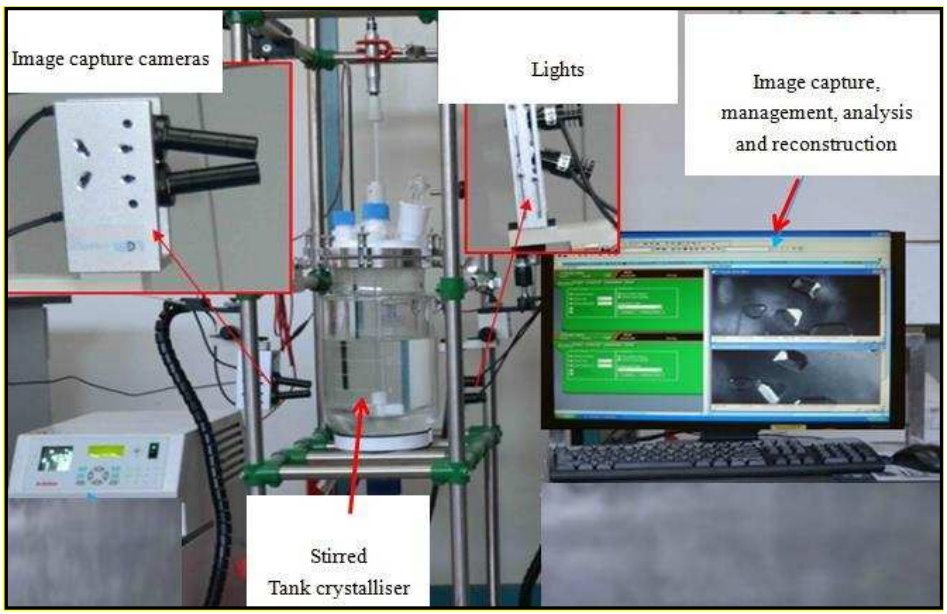

Figure 3. Non-invasive stereo imaging monitoring a 20 Litre stirred tank crystalliser.

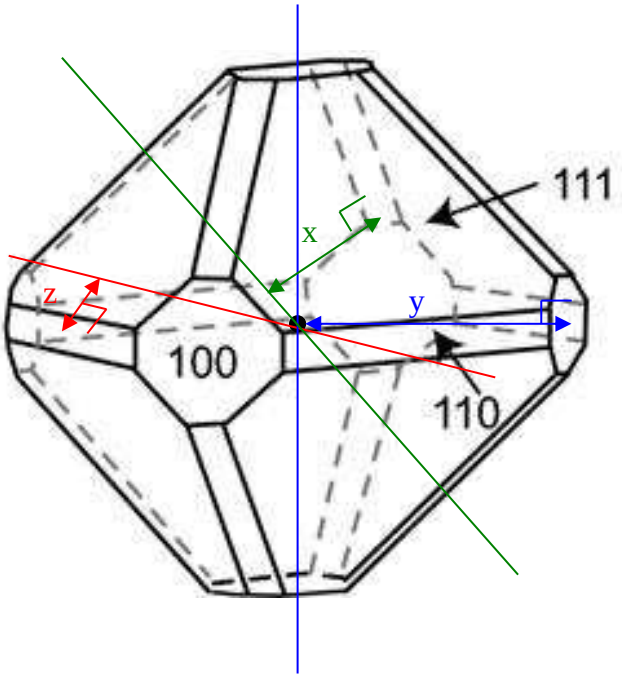

Figure 4. Morphology of a potash alum crystal and the three-size characteristic parameters (x, y, z) to be used in a morphological PB model for face evolution simulation of potash alum crystals [95].

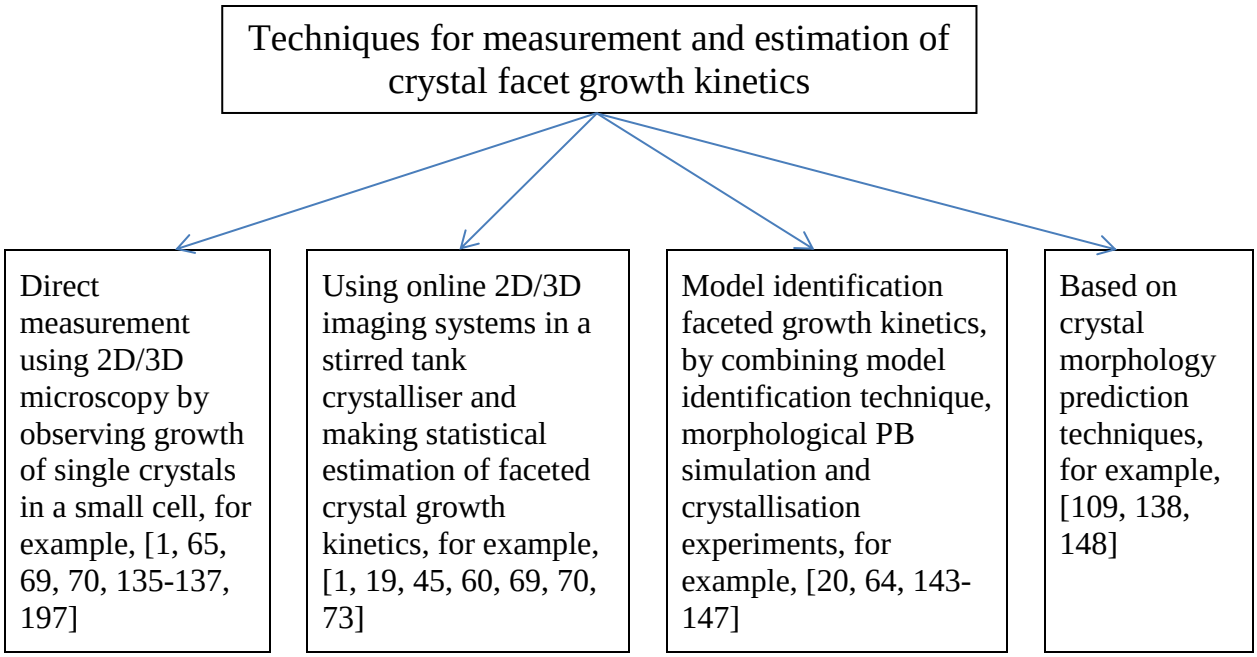

Figure 5.The approaches for the measurements and estimations of faceted crystal growth kinetics.

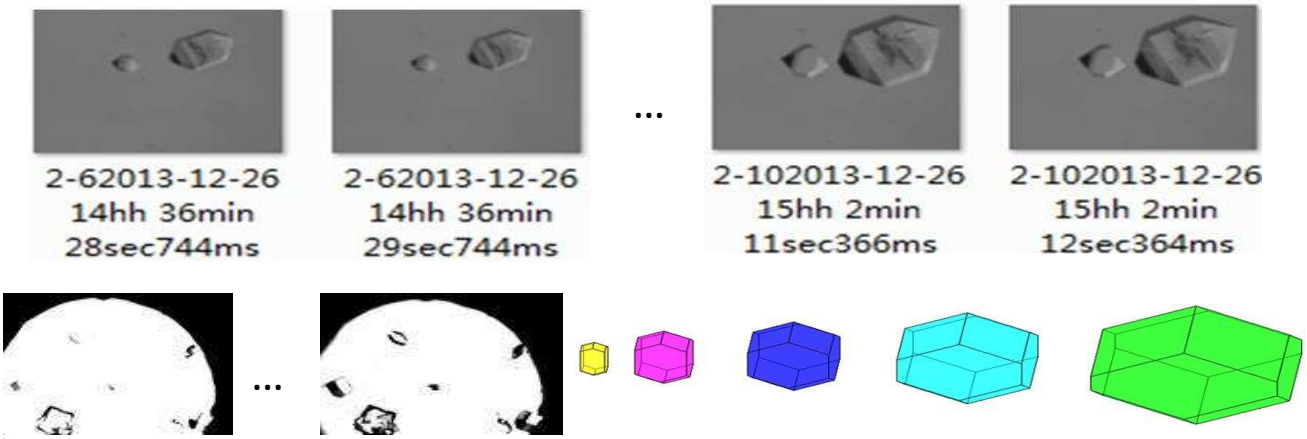

Figure 6. Example images of crystal growth in a cell captured by individual 2D cameras of a stereo vision imaging system for a chemical (top) and a protein (bottom left) and 3D shape reconstructed for the protein crystal (bottom right).